Journal of Biomechanics 129 (2021) 110816

Contents lists available at ScienceDirect

Journal of Biomechanics

journal homepage: www.elsevier.com/locate/jbiomech

A review on the association of thrombus composition with mechanical and radiological imaging characteristics in acute ischemic stroke

Rachel Cahalane [a], Nikki Boodt [b,c,d], Ali Cagdas Akyildiz [a,e], Jo-anne Giezen [e], Manouk Mondeel [e], Aad van der Lugt [b], Henk Marquering [f,g], Frank Gijsen [a,e,*]

[a] Department of Biomedical Engineering, Thoraxcenter, Erasmus MC, University Medical Center Rotterdam, Rotterdam, the Netherlands
[b] Department of Radiology and Nuclear Medicine, Erasmus MC, University Medical Center Rotterdam, Rotterdam, the Netherlands
[c] Department of Neurology, Erasmus MC, University Medical Center Rotterdam, Rotterdam, the Netherlands
[d] Department of Public Health, Erasmus MC, University Medical Center Rotterdam, Rotterdam, the Netherlands
[e] Department of Biomechanical Engineering, Delft University of Technology, Delft, the Netherlands
[f] Department of Radiology and Nuclear Medicine, Amsterdam University Medical Centers, Location AMC, University of Amsterdam, Amsterdam, the Netherlands
[g] Department of Biomedical Engineering and Physics, Amsterdam University Medical Centers, Location AMC, University of Amsterdam, Amsterdam, the Netherlands

ARTICLE INFO

Keywords:
Thrombus
Imaging
Endovascular treatment
Composition
Mechanics

ABSTRACT

Thrombus composition and mechanical properties significantly impact the ease and outcomes of thrombectomy procedures in patients with acute ischemic stroke. A wide variation exists in the composition of thrombi between patients. If a relationship can be determined between the composition of a thrombus and its mechanical behaviour, as well as between the composition of a thrombus and its radiological imaging characteristics, then there is the potential to personalise thrombectomy treatment based on each individual thrombus. This review aims to give an overview of the current literature addressing this issue.

Here, we present a scoping review detailing associations between thrombus composition, mechanical behaviour and radiological imaging characteristics. We conducted two searches 1) on the association between thrombus composition and the mechanical behaviour of the tissue and 2) on the association between radiological imaging characteristics and thrombus composition in the acute stroke setting.

The review suggests that higher fibrin and lower red blood cell (RBC) content contribute to stiffer thrombi independent of the loading mode. Further, platelet-contracted thrombi are stiffer than non-contracted compositional counterparts. Fibrin content contributes to the elastic portion of viscoelastic behaviour while RBC content contributes to the viscous portion. It is possible to identify fibrin-rich or RBC-rich thrombi with computed tomography and magnetic resonance imaging vessel signs. Standardisation is required to quantify the association between thrombus density on non-contrast computed tomography and the RBC content. The characterisation of the thrombus fibrin network has not been addressed so far in radiological imaging but may be essential for the prediction of device-tissue interactions and distal thrombus embolization. The association between platelet-driven clot contraction and radiological imaging characteristics has not been explicitly investigated. However, evidence suggests that perviousness may be a marker of clot contraction.

1. Introduction

Acute ischemic stroke (AIS) treatments focus on the rapid recanalisation of on occluded intracranial artery by pharmacological dissolution and/or mechanical removal of the occluding thrombus. Despite the efficacy of endovascular thrombectomy (EVT) for AIS due to large vessel occlusion (Berkhemer et al., 2015; Campbell et al., 2015; Goyal et al., 2015; Jovin et al., 2015; Saver et al., 2015), substantial reperfusion is

Abbreviations: AIS, Acute Ischemic Stroke; CTA, Computed Tomography Angiography; DSA, Digital Subtraction Angiography; EVT, EndoVascular Thrombectomy; HAS, Hyperdense Artery Sign; HU, Hounsfield Unit; MRI, Magnetic Resonance Imaging; NCC, Non-Contracted Clot; NCCT, Non-Contrast Computed Tomography; PCC, Platelet-Contracted Clot; RBC, Red Blood Cell; SVS, Susceptibility Vessel Sign; WBC, White Blood Cell; IV-rtPA, intravenous recombinant tissue plasminogen activator.

* Corresponding author at: Department of Bioengineering, Erasmus MC, University Medical Center, PO Box 2040 3000 CA, Rotterdam, the Netherlands.
E-mail address: f.gijsen@erasmusmc.nl (F. Gijsen).

https://doi.org/10.1016/j.jbiomech.2021.110816
Accepted 8 October 2021
Available online 15 October 2021

not achieved in 12–56% of cases (Yoo and Andersson, 2017). While the reason for these poor revascularization rates is multifaceted, the nature of the thrombus itself undoubtedly plays a crucial role (Fennell et al., 2018).

Histopathological studies on thrombi retrieved with EVT have shown that thrombi are composed of fibrin, platelets, red blood cells (RBCs), white blood cells (WBCs), lipids and calcification (Almekhlafi et al., 2008; Chueh et al., 2011; Marder et al., 2006; Staessens and De Meyer, 2020). Human thrombi have highly heterogeneous compositions (Chueh et al., 2011; Staessens and De Meyer, 2020), which vary both between patients and within the same thrombus (Alkarithi et al., 2021; Liu et al., 2020b). This composition impacts the outcome of EVT procedures (Brouwer et al., 2018; Choi et al., 2018). Fibrin-rich thrombi require more recanalisation attempts, are associated with longer procedural times and achieve lower revascularization scores (Brinjikji et al., 2017a; Dutra et al., 2019; Maekawa et al., 2018). However, there are currently no guidelines on the preferred use of stent retrievers, aspiration catheters or combined approaches for thrombi based on composition (Powers et al., 2019).

The primary imaging techniques currently used in the setting of AIS are non-contrast computed tomography (NCCT), CT angiography (CTA), magnetic resonance imaging (MRI) and digital subtraction angiography (DSA) (Wintermark et al., 2013). These imaging modalities can provide both qualitative and quantitative information on the thrombus. Thrombus characteristics that have been previously described include dense vessel signs (NCCT and MRI), thrombus density on NCCT, perviousness on CTA and signal intensity on MRI (Liebeskind et al., 2011; Moftakhar et al., 2013; Santos et al., 2016a; Shin et al., 2018).

The role of thrombus composition on the success of EVT is probably mediated by the mechanical properties of the occluding thrombus (Johnson et al., 2017). With stent retrievers or aspiration devices, a wide variety of forces are imposed on the thrombus during the deployment, retraction and removal stages including compressive, tensile, shear and friction forces (Liu et al., 2020a; Mohammaden et al., 2020; Yoo and Andersson, 2017). As the thrombus is integrated into the stent struts or pulled into an aspiration catheter, the ability of the tissue to reshape will depend on its viscoelasticity. Finally, the fracture properties of the thrombus will govern thrombus fragmentation and the occurrence of distal embolization. The mechanical behaviour of the thrombus and the performance of intra-arterial devices are affected by the thrombus composition (Chueh et al., 2011; Yuki et al., 2012).

It has been postulated that personalization of EVT based on the suspected response of the thrombus may lead to better recanalization rates and improved outcomes (Brouwer et al., 2018; Simons et al., 2015). To eventually determine which devices and/or techniques should be, and could be, used with certain thrombus types, two relations must be determined. First, whether there is an association between composition and mechanical properties. If mechanics differ according to thrombus composition, then thrombi with different compositions may benefit from distinct types of devices and/or retrieval strategies. For example, fibrin-rich samples have proven more difficult to retrieve (Yuki et al., 2012) and preliminary in vitro studies demonstrate improved recanalization rates for this thrombi when using specially designed devices (Fennell et al., 2018). If we do determine that certain techniques work better with thrombi of differing compositions, then methods to characterise these thrombi in the setting of AIS stroke must be developed. Therefore the second association that needs to be established is between thrombus composition and admission imaging characteristics. Since EVT has become the standard clinical practice for large vessel occlusion AIS, thrombi have become available for study and there is increasing literature on both topics. This scoping review aims to summarise the findings of these two associations.

2. Results

The scoping review search methods are presented in the supplementary file. Here, we summarise the findings from studies that examined 1) the association between thrombus composition and mechanical characteristics and 2) the association between radiological imaging characteristics and thrombus composition. There are wide variations in the methods of assessing thrombus composition. First, there are variations in terms of experimental methods, including gross pathology (qualitative assessment of histological composition based on the visual appearance of the thrombus) (Fig. 1A), thrombus analog protocols where blood components are reconstituted in predetermined volumetric ratios (Fig. 1B), histological stains (Hematoxylin and Eosin [H&E] and Martius Scarlet Blue [MSB]) (Fig. 1C) and immunohistochemistry (Fig. 1D). Second, there are variations in the histological components that are analysed, including RBCs, fibrin/platelets, fibrin, fibrinogen, platelets, WBCs, lipids and calcium. Third, there are variations in the stains used in the histological and immunohistochemistry approaches. Finally, there are variations in the methods of quantification. Quantitative methods can be subdivided into manual and automatic image analysis. Manual methods involve colour-based classification thresholding while automated methods apply machine learning techniques to segment tissue composition (Orbit Image Analysis). However, most reports categorise samples into RBC-rich, fibrin-rich or mixed thrombi. These categories are not always clearly defined (Chueh et al., 2011) and if they are, there is a lack of uniformity between studies on the definition of RBC-rich, fibrin-rich and mixed thrombi (Brinjikji et al., 2017b; Fitzgerald et al., 2019b; Kirchhof et al., 2003). Moreover, dichotomisation or categorical analysis of thrombus composition reduces statistical power. Where applicable, we have detailed assessment methods of thrombus composition in the tables.

2.1. Thrombus composition and mechanics

Two methods of studying the association between thrombus composition and mechanical characteristics have been observed. Experiments with human material such as thrombi from EVT procedures or thrombi dissected from tissue sources known to contribute to AIS (i.e. carotid plaques) are most relevant for clinical practice. However, thrombi removed by EVT procedures will have undergone supraphysiological loading and the properties characterised ex vivo may not accurately reflect the in vivo state. Additionally, any thrombi that were successfully dissolved by thrombolysis or could not be retrieved with EVT procedures cannot be included in the analysis. Therefore, the majority of studies utilise thrombus analogs (or in vitro thrombi) (Duffy et al., 2017; Liu et al., 2020a). The advantages of this method include the ability to produce homogeneous analogs in a largely controllable composition and shape to conduct reproducible mechanical characterisation experiments (Johnson et al., 2017). However, the formation of in vitro thrombi in static conditions does not represent the dynamic environment in which thrombi are formed within the human body. Additionally, there is also no clear consensus on the blood of which species should be used in these experiments. In these studies, in vitro or ex vivo thrombi are subject to mechanical evaluation using different loading modes: tension and compression. The viscoelastic behaviour is primarily evaluated using rheometry. The friction and fracture properties are also evaluated. Fig. 2 summarises the mechanical loading that is relevant in the context of EVT procedures. Experimental conditions and results are detailed in Tables 1-3.

2.1.1. Compression

Six in vitro studies examined the unconfined compressive properties of thrombus analogs, two studies examined the unconfined compressive properties of ex vivo human thrombi and one in vitro study conducted indentation experiments. There is a wide variation in the properties reported for thrombi tested in unconfined compression, as illustrated in Table 1. This makes it difficult to directly compare studies.

A linear stress–strain response is reported for thrombi formed from platelet-rich and platelet-poor plasma (producing platelet-contracted

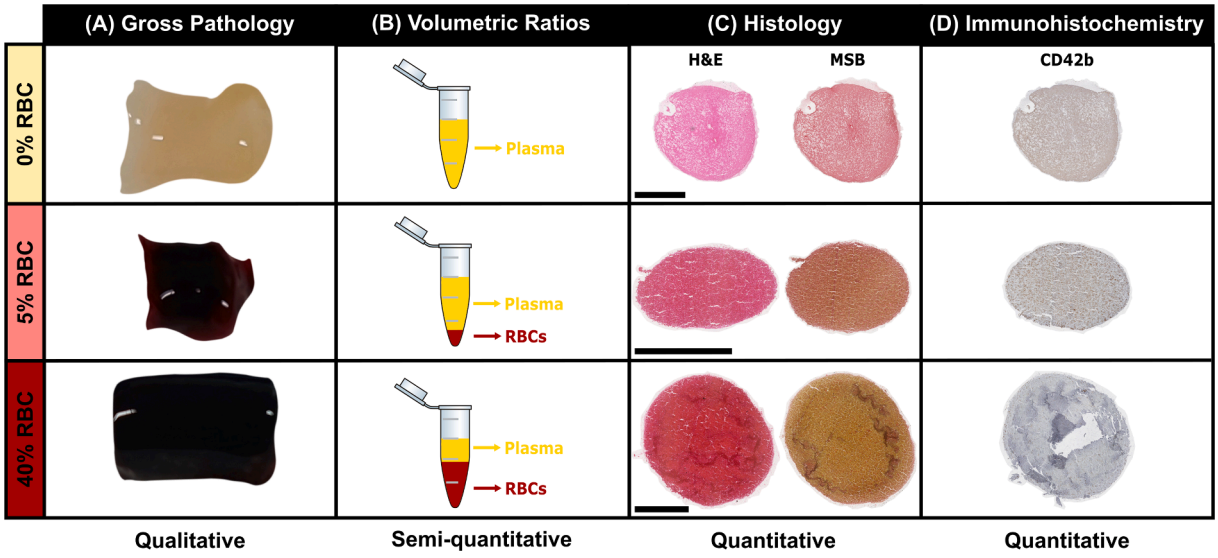

Fig. 1. Overview of the primary methods used to assess thrombus composition: (A) gross pathology, (B) known from thrombus analog protocols where blood components are reconstituted in predetermined volumetric ratios, (C) histology (for example Hemotoxylin and Eosin (H&E) and Martius Scarlet Blue (MSB) staining), (D) immunohistochemistry (for example CD42b platelet marker). All scale bars represent 1mm. All figures depict 0% (platelet-rich), 5% and 40% red blood cell thrombus analogs.

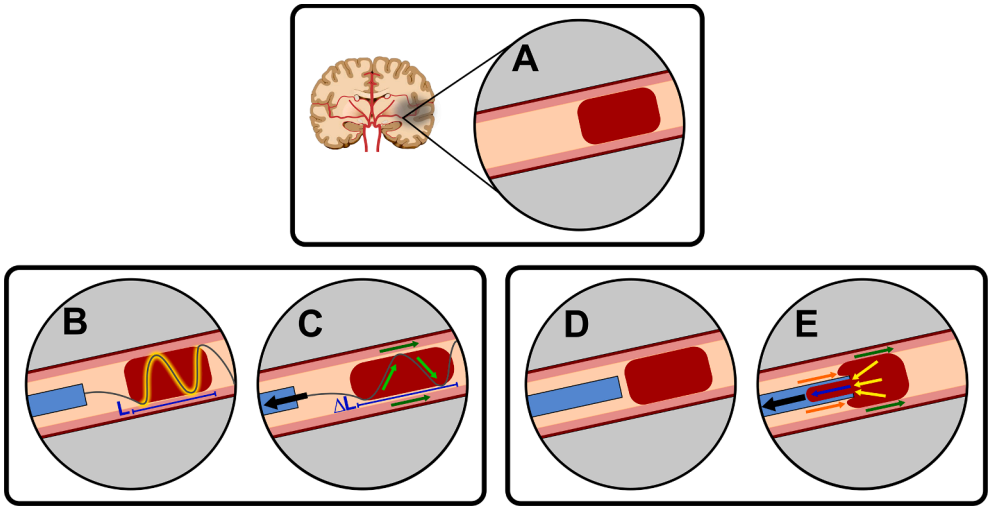

Fig. 2. Mechanical loading conditions associated with endovascular retrieval techniques. (A) Occluding thrombus in a vessel. (B) Stent retriever deployment: the stent struts compress the thrombus and additional embedding depth can be achieved over time (yellow segment) (Weafer et al., 2019). (C) Stent retriever retraction: frictional and adhesion forces exist between the thrombus and the vessel wall (dark green arrows) (Gunning et al., 2018; Yoo and Andersson, 2017) and the thrombus and the device (light green arrows), a tensile force can be imposed on the thrombus as it is retrieved (blue ΔL), which may induce thrombus fracture (Liu et al., 2020a,b). (D) Aspiration catheter. (E) Negative pressure applied: frictional and adhesion forces exist between the thrombus and the vessel wall (dark green arrows) (Gunning et al., 2018; Yoo and Andersson, 2017), the thrombus must compress and elongate to fit within the aspiration catheter (yellow and blue arrows) (Yoo and Andersson, 2017) and the thrombus viscoelasticity and shear behaviour will determine how the thrombus deforms to fit within the catheter (orange arrows) (Yoo and Andersson, 2017).

clots [PCC] and non-contracted clots [NCC], respectively) between 33 and 50% compressive strain (Liang et al., 2017). All other thrombus analogs exhibited non-linear stress–strain behaviour in unconfined compression analysis. Fibrinogen concentration is positively associated with the elastic moduli of thrombi for both healthy subjects and patient samples (elastic modulus ranging from 0 to 120 kdynes/cm^2) (Carr and Carr, 1995; Dempfle et al., 2008). Machi et al. (2017) also determined that the force required to compress fibrin-rich samples to 50% of their height is 13 times higher than that of RBC-rich thrombus analogs. Interestingly, a non-linear dependence of compressive stiffness on RBC content was observed in the studies of Johnson et al. (2019) and Johnson et al. (2020). Similarly, whole blood clots (approximately 45% RBC) were stiffer than both PCC and NCC (Liang et al., 2017). Unconfined compression tests on PCC and NCC revealed that PCC are stiffer than NCC (Liang et al., 2017) for all degrees of RBC concentration (Johnson et al., 2019). PCC also have earlier onset points (the strain at which the material transitions from low-stiffness to high-stiffness behaviour) than NCCs (Johnson et al., 2019). Importantly, clot contraction was found to affect the mechanical properties of the thrombi, but not the composition (Johnson et al., 2019). Clot elastic modulus is a linear function of platelet concentrations (Carr and Carr, 1995). In an indentation study, Weafer et al. (2019) characterised the compressive clot stiffness of thrombus analogs. The indenter tip was shaped to simulate a single strut of a stent retriever as in the real-life stent retriever deployment (a rectangular surface of 3 mm × 0.075 mm contacting the clot). The initial thrombus compressive stiffness upon indentation was inversely related to RBC concentration. Higher RBC concentration was also associated with a greater maximum indentation depth due to the lower stiffness of these samples.

Only two studies examined the unconfined compressive properties of

Table 1
Studies that assessed the association between thrombus composition and compressive properties.

Study (Year)	Type	Species	n	Testing Protocol	Properties Reported	Composition Method	Composition Analysis	Stress-Strain Behaviour	Results
Carr and Carr (1995)	in vitro (static)	Human	15	Unconfined compression: not described	Elastic modulus (no strain defined)	Volumetric ratios	Quantitative: fibrinogen (0.5, 1, 2, 3, 4, 5 mg/mL), platelet (0, 25, 50, 75, 100, 175 $\times 10^3$ /μL) and RBC (0%, 20%, 40%) concentrations	Not reported	Clot elastic modulus is a linear function of both fibrinogen and platelet concentrations. Elastic modulus increased at 40% RBC concentration.
Dempfle (2008)	in vitro (static)	Human	552 [a]	Unconfined compression: not described	Elastic Modulus (no strain defined)	Clauss assay	Quantitative: fibrinogen concentration	Not reported	Increasing fibrinogen concentration increases the elastic modulus of the clot ($F = 185.4$, $p < 0.0001$).
Machi (2017)	in vitro (static)	Human	2	Unconfined compression: 50% strain	Mean radial force at 50% strain over 5 cycles	Volumetric ratios	Qualitative: white (PCC) and red (WB)	N/A	White clots were 13 times stiffer than red clots (force required 9 mN/mm^2 vs. 0.7 mN/mm^2).
Liang (2017)	in vitro (static)	Human	3	Unconfined compression: to $\varepsilon_{33\%}$ or $\varepsilon_{50\%}$ at 10 μm/s	Tangent stiffness at 33% and 50% strain	Volumetric ratios	Qualitative: PCC, NCC and WB	Linear response for NCC and PCC from $\varepsilon_{33\%}$ to $\varepsilon_{50\%}$. Non-linear response for WB clots from $\varepsilon_{33\%}$ to $\varepsilon_{50\%}$.	Whole blood clots were stiffer than both PCC and NCC at $\varepsilon_{33\%}$ (9 vs. 2 and 1 kPa) and $\varepsilon_{50\%}$ (21 vs. 4 and 2 kPa).
Johnson (2019)	in vitro (static)	Ovine	8	Unconfined compression: Force ramp to 15 N at a rate of 0.5 N/min	Low strain stiffness (initial 10%), high strain stiffness (final 2%) and the onset point	Histology: MSB	Quantitative: percent fibrin and RBCs	Non-linear	PCCs were found to be stiffer than NCCs with earlier onset points, across all hematocrits. However, the compositional analysis of PCC and NCC for the same % RBC show little difference. A non-linear dependence on hematocrit was observed.
Weafer (2019)	in vitro (static)	Ovine	5	Indentation: 1.5mN pre-load, loading at 1.5 mm/min to 12.5 mN load	Compressive stiffness	Volumetric ratios	Semi-quantitative: 0% high density, 0% low density, 5%, 40% and 80% RBC	N/A	The initial thrombus compressive stiffness upon indentation was inversely related to RBC concentration.
Johnson (2020)	in vitro (static)	Ovine	4	Unconfined compression: nominal strain of 80% at a constant strain-rate of 10%/s	Peak stress at 80% compression. Tangent stiffness at 10%, 50% and 80% strain.	Volumetric ratios	Semi-quantitative: 0%, 5%, 40% RBC and WB	Non-linear	5% RBC had the greatest peak stress following by 0%, WB and 40%. At low strains (<30%), 0% RBC had the largest stiffness (followed by 5%, WB and 40%, in the order of 1 kPa [$E_{10\%}$]). At high strains (>30%), 5% RBC had the largest stiffness (followed by 0%, WB and 40% in the order of 10 kPa [$E_{50\%}$] and 100 kPa [$E_{80\%}$]).
Chueh (2011)	ex vivo (aspiration and carotid plaques)	Human	9 and 13	Unconfined compression: pre-load 0.0001 N, force ramp from 0.0001 to 15 N at 0.5 N/min	The onset point and secant stiffness at strains of 0–45%, 0–75% and 75–95%	Histology: H&E, MSB	Qualitative: calcified (large amounts of calcium-phosphate apatite), aged (dark reddish-	Non-linear	Calcified thrombi exhibited the largest $E_{0\text{-}45\%}$ (0.63 MPa) compared with aged (0.17 MPa) and red samples (0.026 MPa). Calcified

(*continued on next page*)

Table 1 (*continued*)

Study (Year)	Type	Species	n	Testing Protocol	Properties Reported	Composition Method	Composition Analysis	Stress-Strain Behaviour	Results
							brown colour) and red thrombi (high amounts of RBCs)		thrombi had earlier onset points (43%) compared with aged and red thrombi (85% and 91%).[b] Calcified thrombi exhibited the highest stress values while red thrombi exhibited the highest strain values.
Boodt (2021)	ex vivo (stent retriever)	Human	41	Unconfined compression: 80% strain at a rate of 10%/s	Tangent stiffness at 75% strain	Histology: H&E Immunohistochemistry: CD61	Quantitative (automatic): fraction of fibrin, RBCs, platelets and WBCs	Non-linear	F/P were associated with increased $E_{75\%}$ (aβ, 9 [5–13]) kPa. RBCs were associated with decreased $E_{75\%}$ (aβ, −9 [-13 to −5]) kPa. High platelet values (>70%) were strongly associated with increased $E_{75\%}$ (aβ, 56 [38–73]).

N for in vitro studies indicates the number of types of thrombus analogs examined, except where otherwise indicated. Where values were not explicitly reported in the studies, results have been approximated from the figures. $E10_{\%}$, tangent stiffness at 10% strain; $E_{50\%}$, tangent stiffness at 50% strain; $E_{75\%}$, tangent stiffness at 75% strain; $E_{80\%}$, tangent stiffness at 80% strain; $E_{0\text{-}45\%}$, secant stiffness between 0 and 45% strain; F/P, fibrin/platelet; H&E, Hematoxylin and Eosin; MSB, Martius Scarlet Blue; NCC, Non-Contracted Clot; PCC, Platelet-Contracted Clot; RBC, Red Blood Cell; WB, Whole Blood; $\varepsilon_{33\%}$, 33% strain; $\varepsilon_{50\%}$, 50% strain.

[a] Number of patient blood samples used to make in vitro thrombi.

[b] Mean values presented.

thrombi extracted from AIS patients. All the samples exhibited non-linear stress–strain behaviour. Chueh et al. (2011) categorised thrombi retrieved from aspiration procedures or dissected from carotid plaques as either calcified, red or aged. Calcified thrombi had a lower onset point (42.9 ± 8.0%) compared with aged and red thrombi (85.4 ± 0.9% and 91.29 ± 0.82%). Calcified thrombi also exhibited the largest secant stiffness ($E_{0\text{-}45\%}$: 0.63 ± 0.38 MPa) compared with aged (0.17 ± 0.039 MPa) and red samples (0.026 ± 0.0026 MPa). The $E_{0\text{-}75\%}$ and $E_{75\text{-}95\%}$ values for (calcified) thromboemboli were 0.04 ± 0.01 and 0.43 ± 0.06 MPa, and for non-calcified thrombi dissected from carotid plaques were 0.11 ± 0.037 and 1.60 ± 0.50 MPa, respectively. Boodt et al. (2021) quantified the proportion of fibrin, RBCs, platelets and WBCs in thrombi acquired from stent retrieval procedures. In multivariate regression analysis, $E_{75\%}$ was positively associated with F/P content (aβ, 9 [5–13] kPa) and negatively associated with RBCs (aβ, −9 [-13 to −5] kPa). The authors also observed a strong positive association between platelet content and $E_{75\%}$, but for high platelet contents only (>70%). The average $E_{75\%}$ in the study of Boodt et al. (2021) was 122 ± 104 kPa, compared with an $E_{0\text{-}75\%}$ range of 10 to 65 kPa in the study of Chueh et al. (2011). The fact that all samples in the study of Chueh et al. (2011) were acquired from aspiration procedures and qualitatively characterised as 'red' compared with samples acquired from stent-retrieval procedures in the study of Boodt et al. (2021) with a wide variation in histological composition, may have contributed to the increased stiffness in the latter study.

From these studies, it can be concluded that thrombus analogs have lower low-strain stiffness compared to ex vivo thrombus data. The high-strain behaviour of thrombus analogs is similar to the data from aspirated thrombi in the study of Chueh et al. (2011) but lower than the data from thrombi removed using stent retrievers (Boodt et al., 2021). It should also be noted that thrombus composition cannot account for all the variation observed in the mechanical properties of ex vivo thrombi (Boodt et al., 2021; Chueh et al., 2011).

2.1.2. Tension

One in vitro study describes the association between tensile stiffness and thrombus composition (Liu et al., 2020a). Human thrombus analogs exhibited a variation in the nominal stress–strain behaviour, some samples were high non-linear while others appear closer to linear behaviour. There is also a wide range of values reported for $E_{0.45}$ (11 – 114 kPa). $E_{0.45}$ had a strong positive correlation with fibrin concentration ($r = 0.613$, $p < 0.001$), a strong negative correlation with RBC concentration ($r = -0.609$, $p < 0.001$) and a moderate positive correlation between platelet concentration and $E_{0.45}$ ($r = 0.349$, $p = 0.013$) (Liu et al., 2020a).

When comparing the tensile and compressive properties of thrombus analogs and ex vivo specimens it is clear that exact comparisons are difficult to make due in part to the different properties that are reported, the wide range of values obtained and the differences in the histological composition of the samples. Additionally, tensile stiffness values have only been acquired for thrombus analogs in one study. The fewer number of studies conducted in tension is likely due to the difficulties in the handling of thrombus specimens required for tensile analysis (Johnson et al., 2017; Liu et al., 2021). However, some general trends are observed. Higher fibrin and lower RBC content contribute to stiffer thrombi both in tensile (Liu et al., 2020a) and compressive loading (Boodt et al., 2021; Fereidoonnezhad et al., 2021). Additionally, thrombi contracted by platelets are stiffer in compression (Boodt et al., 2021; Johnson et al., 2019), and a moderate positive correlation was also found between tensile stiffness and fraction of platelets within thrombus analogs in tension (Liu et al., 2020a). Thrombus analogs with similar composition in tension appear to have slightly higher stiffness values for comparable samples in compression (Johnson et al., 2020; Liu et al., 2020a). This may be attributed to the histological assessment of composition in the tensile study (Liu et al., 2020a) compared with the in vitro protocol compositional ratios used in the compression study (Johnson et al., 2020), which may underestimate the true RBC content of the samples (Duffy et al., 2017). Finally, experiments conducted for material parameter estimation in the study of Fereidoonnezhad et al. (2021) demonstrate compression-tension asymmetry for 5% RBC samples. Further work is required here to uncover the compression-tension asymmetry for other compositions.

Table 2
Studies that assessed the association between thrombus composition and viscoelastic properties.

Study (Year)	Type	Species	n	Testing Protocol	Properties Reported	Composition Method	Composition Analysis	Results
Tynngård (2006)	in vitro (static)	Human	15	Rheometry (not described)	The change in elasticity (G') over time	Known from thrombus analog protocols	Semi-quantitative: 0, 10, 30, 50, 100 and 200 $\times 10^9$ platelets/L, PCC and NCC, original fibrinogen or + 2 or + 4 g/L fibrinogen, 0%, 20%, 30% or 40% RBC	Increasing number of platelets and fibrinogen concentration gave higher elasticity values while increasing haematocrit gave lower elasticity values. PCC have higher elasticity values compared with NCC.
Gersh (2009)	in vitro (static)	Human	7	Rheometry: a strain-controlled dynamic time sweep test was performed with a frequency of 5 rad/s, 2% strain	Elastic (G'), viscous modulus (G'') and ratio of viscosity to elasticity (tan δ)	Volumetric ratios	Semi-quantitative: 0, 5, 10, 20, 30, 40, or 50% RBCs	Samples with RBC exhibited biphasic behaviour of G' and G'' at a threshold of 10% RBC. Addition of any amount of RBCs will influences clot viscoelasticity by increasing the viscous component of the sample relative to the elastic.[a]
Huang (2011)	in vitro (static)	Porcine	3	Instantaneous force approach: 1 MHz ultrasound transducer, sphere displacement detected using a 20 MHz transducer	Shear modulus (G') and viscosity (G'')	Volumetric ratios	Semi-quantitative: 0, 20 or 40% RBC	G' decreasing with increasing RBC content (0%: 620 ± 81 Pa and 40%: 173 ± 52 Pa [40%]). G'' increased with increasing RBC content (0%: 0.16 ± 0.06 Pa•s and 40%: 0.32 ± 0.07 Pa•s).[a]
van Kempen (2016)	in vitro (static)	Porcine	3	Rheometry. Linear viscoelasticity: the frequency of the oscillation is increased from 0.63 to 63 rad/s, with 0.01 strain amplitude. Nonlinear viscoelasticity: (LAOS) strain amplitude is increased from 0.01 to 1.	Linear: elastic (G') and viscous moduli (G''). Non-linear: softening, strain stiffening and nonlinear viscous dissipation.	Known from thrombus analog protocols	Qualitative: PCC, NCC and WB	G' and G'' of PCC are slightly higher than WB and much higher than NCC. Softening: more pronounced for WB compared to PCC and NCC. Strain stiffening: more pronounced for NCC compared with PCC and WB. Nonlinear viscous dissipation: more pronounced for NCC compared with PCC and WB.
Liang (2017)	in vitro (static)	Human	3	Compression-decompression cycles. Rheometry: constant oscillatory strain of 3.3% at a frequency of 1.5 Hz to produce a linear shear stress response to imposed shear strain.	Hysteresis area. Shear storage (G′) and loss moduli (G″) as a function of strain	Known from thrombus analog protocols	Qualitative: PCC, NCC and WB	Hysteresis area of WB was largest (5.52), followed by PCC (2.02) and NCC (1.10). PCC have a higher G' compared with NCC, and become stiffer after loading. For both PCC and NCC, stiffness increased after each cycle. For WB clots, the stiffness decreased after the initial cycle.
Weafer (2019)	in vitro (static)	Ovine	5	Indentation: a constant force of 12.5 mN for 5 mins	Creep	Volumetric ratios	Semi-quantitative: 0% high density, 0% low density, 5, 40 and 80% RBC	The highest amount of additional embedding depth was achieved for 0% high density clots (36 ± 17% additional depth versus ~ 10 %[a] for 40% RBC over 5 mins).
Johnson (2020)	in vitro (static)	Ovine	4	Cyclic unconfined compression (10 cycles) and stress relaxation (60% strain for 1000 s)	Hysteresis and percentage stress relaxation	Volumetric ratios	Semi-quantitative: 0, 5 and 40% RBC and WB	Loading-unloading hysteresis demonstrated for all samples. Lower RBC content was associated with greater stress relaxation (0%: 97 ± 5% and 5%: 89 ± 8%) than those with higher RBC concentration (40%: 54 ± 20% and WB: 63 ± 19%).
Liu (2021)		Human	2					

(*continued on next page*)

Table 2 (*continued*)

Study (Year)	Type	Species	n	Testing Protocol	Properties Reported	Composition Method	Composition Analysis	Results
	in vitro (static)			Rheometry: oscillatory strain (1%, 1 Hz)	Storage (G') and loss moduli (G'')	Known from thrombus analog protocols	Qualitative: NCC and WB	Storage and loss moduli of WB clots is larger than that of PPP clots (G': 303 ± 80 vs. 128 ± 45 Pa and G'': 14 vs. 3 Pa).
Chueh (2011)	ex vivo (aspiration and carotid plaques)	Human	9 and 13	Unconfined compression: 60% strain for 5 mins followed by a recovery period of 15 mins	Strain Recovery (%)	Histology: H&E, MSB	Qualitative: calcified, aged and red	Red thrombi from aspiration procedures recovered 33 ± 2% of their strain. Strain recovery could not be determined for calcified samples due to the high force required. Strain recovery could not be measured for aged samples due to fragmentation.

N for in vitro studies indicates the number of types of thrombus analogs examined. H&E, Hematoxylin and Eosin; LAOS, Large Amplitude Oscillatory Shear; MSB, Martius Scarlet Blue; NCC, Non-Contracted Clot; PCC, Platelet-Contracted Clot; RBC, Red Blood Cell; WB, Whole Blood.

[a] Only platelet-poor plasma used.

2.1.3. Viscoelasticity

Eight in vitro studies and one ex vivo study examined the viscoelastic properties of thrombi (Table 2). Studies that conducted cyclic analysis confirmed loading–unloading hysteresis for all samples (Johnson et al., 2020). The hysteresis area for WB clots was the largest (5.52), followed by PCC (2.02) and NCC (1.10) (Liang et al., 2017). Johnson et al. (2020) also performed compressive stress relaxation experiments on thrombus analogs. All samples exhibited significant stress relaxation. Thrombi with lower RBC concentration demonstrated greater stress relaxation than those with higher RBC concentration (0%: 97 ± 5% and 5%: 89 ± 8% vs. (40%: 54 ± 20% and WB: 63 ± 19%). Similarly, Weafer et al. (2019) examined the creep response of thrombus analogs with varying RBC concentration by applying a constant force via an indenter tip in the profile of a single stent strut. The degree of creep (additional depth) decreased with increasing thrombus RBC concentration: 0% high density clots (36 ± 17% additional depth versus ~ 10% for 40% RBC over 5 mins) (Weafer et al., 2019).

Six studies examined the viscoelastic properties of thrombus analogs using rheometry (Gersh et al., 2009; Liang et al., 2017; Liu et al., 2021; Tynngård et al., 2006; van Kempen et al., 2016) or an instantaneous force approach (Huang et al., 2011) to determine either the elastic (G') and viscous (G'') moduli. Both G' and G'' moduli were found to be dependent on RBC concentration. An increase in the RBC content decreased the elastic portion (Gersh et al., 2009; Huang et al., 2011; Tynngård et al., 2006) while increasing the viscous portion (Gersh et al., 2009; Huang et al., 2011). PCC were also found to have higher moduli than NCC (Liang et al., 2017; Tynngård et al., 2006; van Kempen et al., 2016). In terms of non-linear viscoelastic behaviour, van Kempen et al. (2016) described three features: softening, strain stiffening and non-linear viscous dissipation using large amplitude oscillatory shear deformation. WB clots exhibit higher softening behaviour compared with PCC and NCC. NCC display larger strain stiffening and non-linear viscous dissipation compared with PCC and WB thrombi.

Chueh et al. (2011) performed compressive stress relaxation experiments on ex vivo thrombi. Red thrombi recovered 32.9 ± 2.3% of their strain. However, the authors were unable to determine the strain recovery of aged and calcified thrombi due to the fragmentation and high stiffness of the samples, respectively.

2.1.4. Friction

Gunning et al. (2018) characterised the frictional properties of ovine thrombus analogs (0%, 5%, 20%, 40%, 80% RBC) using a custom-made apparatus to determine the tangent of the angle at which the samples start to slide on a polytetrafluoroethylene plate. Thrombus composition was found to affect the frictional properties. The authors suggest a threshold of 20% RBC; fibrin-rich thrombus have much higher coefficients of friction (0.51 ± 0.19 [0%] and 0.35 ± 0.13 [5%]) than higher RBC concentration (0.26 ± 0.09 [20%], 0.21 ± 0.06 [40%] and 0.25 ± 0.05 [80%]). The cut-off of 20% RBC was validated by determining that the coefficient of friction for a 0% RBC (~4.4) was still approximately three times higher than that of a whole blood clot (~1.4) on the luminal surface of a bovine aorta.

2.1.5. Fracture

Five in vitro studies and one ex vivo study examined the fracture properties of thrombi (Table 3). Fibrinogen concentration is positively associated with the ultimate tensile strength (Janis et al., 2001; Liu et al., 2020a) and the ultimate tensile strain (Liu et al., 2020a; Luo et al., 2012) of thrombus analogs. Liu et al. (2020a) also examined RBC and platelet concentrations. RBC content is strongly negatively correlated with ultimate tensile strength and moderately negatively correlated with the ultimate tensile strain. The authors also found a moderate positive correlation between the ultimate tensile strength of samples and the platelet concentration. In comparison to thrombi retrieved from large vessel occlusion patients, fibrin and RBC were strongly positively and moderately negatively associated with the ultimate tensile strength of thrombi. Only platelet content was positively correlated with the ultimate tensile strain of ex vivo samples (Liu et al., 2020b). At fracture, the ultimate tensile stress of ex vivo samples ranged from 63 to 2396 kPa and the ultimate tensile strain ranged from 1.05 to 4.89. These values are higher than those acquired for the thrombus analogs (the ultimate tensile stress ranged from 16 to 949 kPa and the ultimate tensile strain ranged from 0.81 to 1.36). Four different fracture patterns were identified from thrombi: focal, multifocal, cavitated, or stress-concentrated (locally at pulling clamp) fractures (Liu et al., 2020b). However, no clear association was found between fracture patterns and histological composition. Fereidoonnezhad et al. (2021) and Liu et al. (2021) examined the fracture toughness and fracture energy of thrombus analogs, respectively. A significant decrease in the fracture toughness of specimens was found with increasing RBC content: 5% (0.022 kJ/m^2), 20% (0.017 kJ/m^2) and 40% (0.007 kJ/m^2). The fracture energy of WB clots is significantly higher than that of NCC (5.90 ± 1.18 vs. 0.96 ± 0.90 J/m). Collectively, these data indicate that RBC-rich clots are more susceptible to fragmentation compared with clots that have a higher fibrin content. A comparison of the fracture resistance of the PCC from the study of Fereidoonnezhad et al. (2021) compared with that of the NCC from the study of Liu et al. (2021) suggests that clot contraction also plays an important role in fracture resistance of thrombi. This must

Table 3
Studies that assessed the association between thrombus composition and fracture properties.

Study (Year)	Type	Species	n	Testing Protocol	Properties Reported	Composition Method	Composition Analysis	Results
Janis (2001)	in vitro (static)	Swine	3	Uniaxial tension, pulled at a rate of 2 mm/s	σ_{UT}	Known from thrombus analog protocols	Semi-quantitative: 300 or 1000 mg/dL fibrinogen, WB	σ_{UT} increased in proportion to the 300 or 1000 mg/dL fibrinogen concentration (2 vs. 7 kPa, respectively). σ_{UT} for WB clots were highly variable.
Luo (2012)	in vitro (static)	Swine	4	Manual elongation	Percent elongation at fragmentation	Known from thrombus analog protocols	Semi-quantitative: 0, 50, 100 and 200 mg fibrinogen dose	The % elongation at fracture increased with increasing fibrinogen dose: 0 mg (160%), 50 mg (170%), 100 mg (191%) and 200 mg (211%), $p < 0.01$.
Liu (2020a)	in vitro (static)	Human	10	Uniaxial tension, pulled at a rate of 0.3 mm/s	σ_{UT} and ε_{UT}	Known from thrombus analog protocols. Confirmed with histology: H&E and immunohistochemistry: CD61	Quantitative: percent RBC, platelets and fibrin	σ_{UT} is strongly positively correlated with fibrin ($r = 0.702$, $p < 0.001$), strongly negatively correlated with RBC ($r = -0.696$, $p < 0.001$) and moderately positively correlated with platelet ($r = 0.395$, $p < 0.001$). ε_{UT} is moderately positively correlated with fibrin ($r = 0.555$, $p < 0.001$) and moderately negatively correlated with RBC ($r = 0.536$, $p < 0.001$).
Fereidoonnezhad (2021)	in vitro (static)	Ovine	3	Notched specimen, pulled at a rate of 10 mm/min	G_{IC}	Volumetric ratios	Semi-quantitative: 5%, 20% and 40% RBCs	Significant decrease in G_{IC} increasing RBC content: 5% (0.022 kJ/m^2), 20% (0.017 kJ/m^2) and 40% (0.007 kJ/m^2).
Liu (2021)	in vitro (static)	Human	2	Modified lap-shear (strain rate: 20/min) and modified double-cantilever beam (3 mm/min)	Fracture energy	Known from thrombus analog protocols	Qualitative: WB and NCC	The fracture energy of WB and NCC clots is 5.90 ± 1.18 J/m^2 and 0.96 ± 0.90 J/m^2, respectively, independent of loading condition.
Liu (2020b)	ex vivo	Human	16	Uniaxial tension, pulled at a rate of 0.2 mm/s	σ_{UT} and ε_{UT}	Histology: H&E Immunohistochemistry: CD61	Quantitative: percent RBC, platelets and fibrin	σ_{UT} is strongly positively correlated with fibrin ($r = 0.670$, $p = 0.005$) and moderately negatively correlated with RBC ($r = -0.565$, $p = 0.023$). ε_{UT} is strongly positively correlated with the platelets ($r = 0.608$, $p = 0.012$).

N for in vitro studies indicates the number of types of thrombus analogs examined. Where values were not explicitly reported in the studies, results have been approximated from the figures. G_{IC}, critical strain energy release rate (fracture toughness); H&E, Hematoxylin and Eosin; NCC, non-contracted clot; RBC, Red Blood Cell; σ_{UT}, Ultimate Tensile Stress; ε_{UT} Ultimate Tensile Strain.

be confirmed in future works.

2.2. Imaging and thrombus composition

Two methods of studying the association between admission imaging characteristics and thrombus composition have been observed. First, admission imaging was used to characterise in vivo thrombi. This method carries the advantage of characterising human tissue in the real-life setting of AIS. Second, thrombus analogs were imaged using clinical modalities in an in vitro setup. These analogs pose the advantage of having a controllable and reproducible composition for repeatable imaging characteristic measurements. As previously mentioned, the formation of in vitro thrombi in static conditions does not represent the dynamic environment in which thrombi are formed within the human body and there is also no clear consensus on the blood of which species should be used in these experiments. Fig. 3 presents an overview of the imaging modalities used in the setting of AIS.

2.2.1. Computed tomography

The **hyperdense artery sign** (HAS) is a qualitative measure that can be obtained from non-contrast CT (NCCT) scans. The presence of a HAS is generally defined as an artery with an increased density in comparison to other vessels, such as the contralateral artery. The diagnosis is based on the visual assessment of experienced neuroradiologists (Boeckh-Behrens et al., 2016; Liebeskind et al., 2011; Shin et al., 2018; Simons et al., 2015). More recently, HAS is defined as an artery with a density $\geq$ 50HU (Fitzgerald et al., 2019b, 2019a) or when the difference in density between the thrombus and the contralateral artery is $\geq$ 4HU (Ye et al., 2021). Table 4 presented all studies that examine the association of a HAS and thrombus composition. The presence of a HAS is more commonly associated with RBC-rich thrombi (Liebeskind et al., 2011; Shin et al., 2018; Ye et al., 2021) and mixed thrombi (Liebeskind et al., 2011). Simons et al. (2015) only found significance for RBC proportion equal to fibrin but not RBC-rich, fibrin-rich or organised fibrin thrombi.

Quantitative studies demonstrated that thrombi with a HAS had higher percentages of RBCs than those with an absence of a HAS (Fitzgerald et al., 2019b; Liebeskind et al., 2011; Shin et al., 2018; Ye et al.,

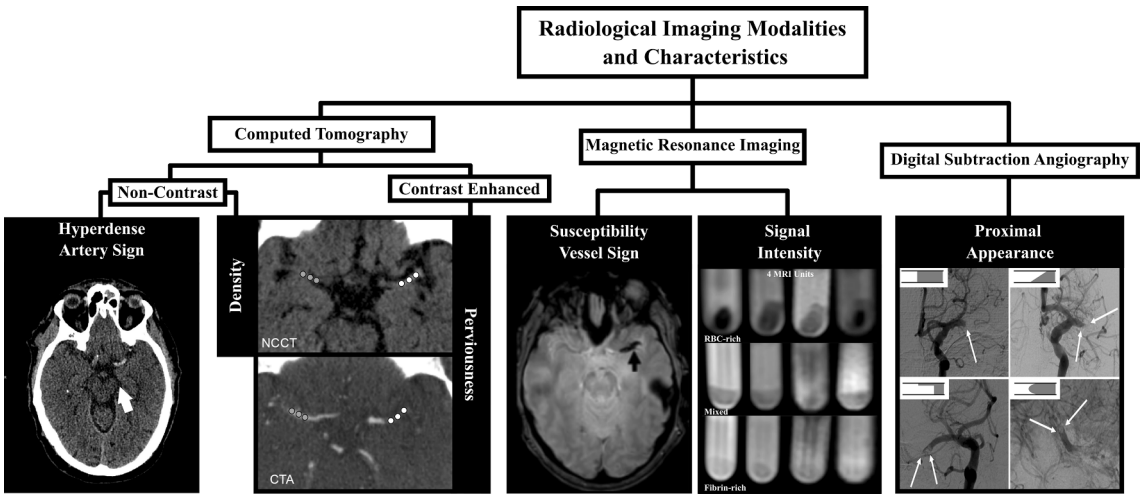

Fig. 3. Overview of radiological imaging modalities and characteristics used in the setting of acute ischemic stroke. Computed tomography: hyperdense artery sign, density and perviousness. Magnetic resonance imaging: susceptibility vessel sign (Darcourt et al., International Journal of Stroke (16, 8) pp: 972-980, Copyright © 2021 by World Stroke Organization, modified by permission of SAGE Publications) and signal intensity (Bourcier et al., Journal of Neuroimaging (27, 6) pp: 577-582, Copyright © 2021 by John Wiley & Sons, Inc., modified by permission of John Wiley and Sons). Digital subtraction angiography: proximal thrombus appearance (adapted by permission from Springer Nature: Springer Clinical Neuroradiology (Angiographic Baseline Proximal Thrombus Appearance of M1/M2 Occlusions in Mechanical Thrombectomy, Mönch), Copyright © (2019)).

Table 4
Studies that assessed the association between thrombus composition and the presence of a hyperdense artery sign on non-contrast computed tomography.

Study	Type	Species	n	HAS Method	Composition Method	Histological Analysis	Results
Liebeskind (2011)	in vivo	Human	20	Visual inspection	Histology: H&E	Quantitative: proportion of fibrin, RBCs and WBCs. Qualitative: RBC-rich, fibrin-rich, mixed (undefined).	%RBC higher with HAS (47% vs. 22%, $p = 0.016$). HAS more common with RBC-rich and mixed categories than fibrin-rich (100% vs. 67% vs. 20%, $p = 0.016$).
Simons (2015)	in vivo	Human	40	Visual inspection	Histology: H&E, CD40	Qualitative: RBC-rich, fibrin-rich, RBC proportion equal to fibrin, organised fibrin (undefined)	A significant association between HAS and RBC proportion equal to fibrin composition ($p < 0.05$).
Boeckh-Behrens (2016)	in vivo	Human	25	Visual inspection	Histology: H&E, EvG	Quantitative: percentage F/P, RBCs and WBCs	The group with HAS showed a higher amount of RBCs (28% vs. 15%, $p = 0.107$).
Shin (2018)	in vivo	Human	37	Visual inspection	Histology: H&E	Semi-quantitative: RBC-rich (RBC outnumbered F/P by > 15%), F/P-rich (F/P outnumbered RBCs by > 15%) and mixed (all others) Quantitative: Percentage F/P, RBCs and WBCs	The presence of a HAS is more commonly associated with RBC-rich thrombi. %RBCs higher with HAS (39% vs. 16% $p = 0.001$).
Fitzgerald (2019a)	in vivo	Human	85	≥ 50HU	Histology: H&E, MSB Immunohistochemistry: CD42b	Semi-quantitative: RBC-rich (≥60% RBCs), fibrin-rich (≥60% fibrin), platelet-rich (≥15.70% fibrin), mixed (all others)	Correlation between platelet-rich thrombi and the absence of a HAS ($\chi^2 = 0.321$, $p = 0.003$).
Fitzgerald (2019b)	in vivo	Human	50	≥ 50HU	Histology: H&E	Semi-quantitative: RBC-rich (≥60% RBCs), fibrin-rich (≥60% fibrin), mixed (all others)	A positive correlation was found between clot composition and the presence of a HAS sign, ($\chi^2 = 6.712$, $p = 0.035$) as well as between RBC-rich thrombi and the presence of a HAS ($\chi^2 = 6.349$, $p = 0.012$).[a]
Ye (2021)	in vivo	Human	53	dHU ≥ 4HU	Histology: H&E, MSB Immunohistochemistry: von Willebrand factor	Semi-quantitative: component considered rich if greater than the all-over median. Quantitative: the proportion of RBC, fibrin and platelets	HAS more associated with RBC-rich clots (62.2% vs. 25.0%, $p = 0.013$). HAS had significantly higher amounts of RBCs (41.1% vs. 20.6%, $p = 0.007$).

dHU, relative thrombus density; EvG, Elastica van Gieson; F/P, fibrin/platelets; HAS, hyperdense artery sign; H&E, Hematoxylin and Eosin staining; MSB, Martius Scarlet Blue staining;, RBC, red blood cell; WBC, white blood cell; dHU, difference in density between the thrombus and the contralateral artery.
[a] Same trend observed for manual readings but was not significant.

2021). Boeckh-Behrens et al. (2016) also observed this trend (but not significantly). A previous *meta*-analysis demonstrated that the mean % RBC in thrombi with a HAS is 45% compared with 23% for those with the absence of a HAS (Brinjikji et al., 2017a). Besides fibrin and RBCs, one study examined the association of platelets and found a significant association between platelet-rich thrombi (≥15.7% platelets) and the absence of a HAS (Fitzgerald et al., 2019a). In general, all in vivo studies found significant (or near significant) associations between the presence of HAS and either the RBC-rich thrombus (qualitative or semi-quantitative) or a higher percentage of RBC (quantitative analysis).

Table 5 presents the findings for **thrombus density**. Thrombus density can be quantified by measuring the density of the thrombus on

Table 5
Studies that assessed the association between thrombus composition and density on non-contrast computed tomography.

Study	Study type	Species	n	Imaging method	CT Slice Thickness (mm)	Density Measurement	Compositional Method	Compositional Analysis	Results
Kirchhof (2003)	in vitro (static)	Human	5	3 ROIs	Not described	Mean HU	Histology: H&E, MSB	Semi-quantitative: red (<10% fibrin), white (<10% RBC) and mixed (all others)	The HU values of red (71 ± 10 and 76 ± 9 HU), white (24 ± 8 HU) and mixed thrombi (36 ± 8 and 52 ± 6 HU) different significantly, $p < 0.05$.
Brinjikji (2017b)	in vitro (6 static, 1 dynamic[a])	Ovine	7	1 ROI	< 2.5	Mean HU	Histology: H&E, MSB	Quantitative: percentage RBCs (99%, 62%, 36%, 18% and low and high density 0% RBC)	Clot attenuation increased with RBC content at all CT energy levels.
Borggrefe (2018)	in vitro (static)	Ovine	3	1 ROI	0.67	Mean HU	Known from thrombus analog protocols	Semi-quantitative: fibrin-rich (0% RBC), RBC-rich (99% RBC) and mixed (35% RBC)	CT density was positively associated with RBC content: fibrin-rich (23.6 ± 1.1 HU), RBC-rich (46.7 ± 1.6 HU) and mixed (34.9 ± 1.6 HU), $p < 0.001$.
Ding (2020)	in vitro (dynamic[b])	Human	5	1 ROI	1	Mean HU	Histology: MSB	Quantitative: relative densities of RBC and F/P	Mean HU values for 75% and 95% RBC were significantly higher than those for 5%, 25% and 50% RBC ($p < 0.001$).
Velasco Gonzalez (2020)	in vitro (static or dynamic[c])	Ovine	9	Multiple ROIs	1	Mean, maximum and minimum HU	Histology: H&E, MSB	Quantitative: percent fibrin, RBCs and WBCs	Max HU values were positively correlated with RBCs ($r = 0.894$, $p < 0.001$), WBCs ($r = 0.608$, $p < 0.001$) and negatively with fibrin ($r = -0.897$, $p < 0.001$).
Niesten (2014)	in vivo	Human	22	3 ROIs	3	Mean (relative) HU	Histology: H&E, MSB	Quantitative: percent RBC, platelets and fibrin	Mean HU values moderately positively correlated with RBC ($r = 0.401$, $p = 0.049$), and weakly negatively correlated with platelets ($r = -0.368$, $p = 0.09$).
Boeckh-Behrens (2016)	in vivo	Human	22	1 ROI	Not described	Undefined	Histology: H&E, EvG	Quantitative: fraction of F/P, RBCs, and WBCs	No significant correlations between HU values and RBCs ($r = 0.255$, $p = 0.253$), F/P ($r = -0.79$, $p = 0.727$) or WBCs ($r = -0.31$, $p = 0.890$).
Sporns (2017)	in vivo	Human	180	Multiple ROIs	Not described	Median (relative) HU	Histology: H&E, EvG, PB Immunohistochemistry: CD3, CD20, CD68	Quantitative: percent RBCs, fibrin, WBCs and other	%RBC positively correlated with rHU values ($r = 0.828$; $p \leq 0.001$). %fibrin inversely correlated with rHU values ($r = –0.795$; $p < 0.001$).
Maekawa (2018)	in vivo	Human	43	1 ROI	5	Mean HU	Histology: H&E	Quantitative: fractions of RBCs, fibrin and WBCs Qualitative: fibrin-rich and RBC-rich (undefined)	%RBC was weakly correlated with thrombus HU values ($r = 0.3$, $p = 0.06$). RBC-rich thrombi had higher HU values than fibrin-rich thrombi (48 vs. 32 HU, $p = 0.04$[d]).
Fitzgerald (2019a)	in vivo	Human	85	Multiple ROIs	Unknown	Mean and maximum HU	Histology: H&E, MSB Immunohistochemistry: CD42b	Quantitative: percent platelets	An inverse correlation observed between %platelets and mean HU ($p = -0.243$, $p = 0.025$).

(*continued on next page*)

Table 5 (*continued*)

Study	Study type	Species	n	Imaging method	CT Slice Thickness (mm)	Density Measurement	Compositional Method	Compositional Analysis	Results
Fitzgerald (2019b)	in vivo	Human	50	Multiple ROIs	Unknown	Mean and maximum HU	Histology: H&E, MSB	Quantitative: percent RBCs, fibrin and WBCs	%RBCs positively corelated with mean HU values ($r = 0.280$, $p = 0.049$[c]).
Songsaeng (2019)	in vivo	Human	54	1 ROI	1.25 or 1.50	Mean HU	Histology: H&E, MSB	Qualitative: red, white and mixed (undefined)	The density of red thrombi (75.5 HU) are significantly higher than those of mixed (60 HU) or white (55 HU), $p = 0.043$ and $p = 0.001$.[d]
Patel (2021)	in vivo	Human	40	2–3 ROIs	0.5	Mean HU	Histology: H&E, MSB	Quantitative: percentage F/P, RBC and WBC	No significant correlations between HU values and %F/P ($r = –0.004$, $p = 0.978$), %RBC ($r = 0.009$, $p = 0.955$) or %WBC ($r = –0.036$, $p = 0.825$).
Ye (2021)	in vivo	Human	53	1 ROI	5 mm	aHU, dHU, rHU	Histology: H&E, MSB Immunohistochemistry: von Willebrand factor	Semi-quantitative: component considered rich if greater than the all over median. Quantitative (automated): the proportion of RBC, fibrin and platelets	dHH and rHU were significantly positively correlated with RBC content ($r = 0.337$, $p = 0.014$ and $r = 0.365$, $p = 0.007$), while aHU was not ($r = 0.146$, $p = 0.296$).

N for in vitro studies indicates the number of types of thrombus analogs examined, except where otherwise indicated. EvG, Elastin van Gieson; F/P, Fibrin/Platelet; H&E, Hematoxylin and Eosin staining; HU, Hounsfield Unit; MSB, Martius Scarlet Blue staining; PB, Prussian Blue; RBC, Red Blood Cells; ROI(s), Region(s) of Interest, rHU, relative HU; WBC, White Blood Cells, aHU, absolute density (mean density); dHU, difference in density between thrombus and contralateral artery; rHU, relative density.

[a] Modified Chandler Loop Technique.

[b] Spun at 20 rpm.

[c] Manual contraction of non-contracted clots using a centrifuge.

[d] Median values.

[e] Histological composition assessed with Adobe Photoshop; $r = 0.291$, $p = 0.040$ when assessed with Orbit Image Analysis.

NCCT in one or multiple small regions of interest in the thrombus. The density as assessed on NCCT is expressed in Hounsfield Units (HU). Because thrombus density measurements are affected by haematocrit, some groups have measured also density in the corresponding collateral artery to calculate a relative density (thrombus density divided by the density of the contralateral artery (Santos et al., 2016b, 2016c) or the difference in density between the thrombus and the contralateral artery (Ye et al., 2021)). Although mean, minimal and maximal densities have been reported, the most recent study identified maximal density as the measure with the greatest accuracy for distinguishing thrombus histology categories (Velasco Gonzalez et al., 2020). Santos et al. (2016c) showed that absolute thrombus density measurement has superior interobserver agreement compared with relative density, and interobserver variation is smaller when multiple ROIs are used. In vitro studies demonstrated that the mean HU values for RBC-rich, fibrin-rich and mixed thrombi are significantly different (Borggrefe et al., 2018; Kirchhof et al., 2003). Ding et al. (2020) found that the mean HU values for 75% and 95% RBC content were significantly higher than the mean HU values for 5%, 25% and 50% RBC content. While thrombus analog density was shown to increase also with increasing RBC content (Brinjikji et al., 2017b), only one in vitro study performed correlative analysis. Velasco Gonzalez et al. (2020) observed that maximum HU values were positively correlated with %RBCs ($r = 0.894$, $p < 0.001$).

Nine clinical studies evaluated thrombus density. Four studies found a relationship between RBC-rich thrombi and increased thrombus density. Two studies found a relationship between RBC-rich thrombi and increased relative thrombus density. Seven studies performed a correlation analysis between quantitative RBC concentration and thrombus density, of which one found a significant positive correlation ($r = 0.8$), two moderate correlations ($r = 0.4$) and two weak correlations ($r = 0.3$) between RBC concentration and thrombus density. These largely positive associations are to be expected as density is linearly correlated with the concentration of haemoglobin (New and Aronow, 1976). However, Patel et al. (2021) and Boeckh-Behrens et al. (2016) reported very different findings: no linear association was found between density and RBC. The only striking difference about this study, and a possible explanation for the conflicting findings, is that the slice thickness (0.5 mm) was smaller than all other studies (1–5 mm). The authors did observe that higher density thrombi (>60HU) had higher amounts of RBC than lower density thrombi (<60HU) (51% vs. 42%), in line with others (Boeckh-Behrens et al., 2016; Borggrefe et al., 2018; Kirchhof et al., 2003), although the findings were not significant. Two studies assessed the correlation between platelet concentration and thrombus density. Niesten et al. (2014) found a weak negative correlation with borderline significance, while Fitzgerald et al. (2019a) found a statistically significant negative correlation.

Perviousness is assessed by subtracting the thrombus' mean density on NCCT from its mean density on CTA. Thereby, perviousness represents the permeability of thrombus for contrast material, measured on single-phase imaging (Berndt et al., 2018; Borggrefe et al., 2018; Santos et al., 2016a). Table 6 presents the studies that assessed the association between thrombus perviousness and composition. An in vitro study found that fibrin concentration was positively associated with contrast uptake after 3 days (Borggrefe et al. 2018). Similarly, two in vivo studies found that permeable thrombi retrieved from AIS patients versus non-permeable thrombi were composed of more fibrin/platelet

Table 6
Studies that assessed the association between thrombus composition and perviousness on non-contrast and contrast-enhanced computed tomography.

Study	Type	Species	n	Imaging Method	Perviousness Method	Compositional Method	Compositional Analysis	Results
Borggrefe (2018)	in vitro (static)	Ovine	3	1 ROI	Increase in HU (undefined)	Known from thrombus analog protocols	Semi-quantitative: fibrin-rich (0% RBC), RBC-rich (99% RBC), mixed (35% RBC)	Contrast enhancement significantly increased after prolonged exposure with fibrin-rich thrombi ($p < 0.05$) and is independently associated with thrombus type ($p < 0.01$).
Berndt (2018)	in vivo	Human	32	Undefined	Increase in HU (undefined)	Histology: H&E	Quantitative: percent F/P, RBC, WBC	Positive correlation with F/P ($r = 0.43$, $p = 0.016$), WBC ($r = 0.34$, $p = 0.06$) and negative correlation with RBC ($r = -0.46$, $p = 0.01$).
Benson et al. (2020)	in vivo	Human	57	Multiple ROIs	Pervious (increase of $\geq$ 10HU) and impervious (increase of $<$ 10HU)	Histology: MSB	Quantitative: relative densities of RBCs, WBCs, fibrin, and platelets. Semi-quantitative: RBC-rich (>49%), WBC-rich (>3.9%), fibrin-rich (>28.7%), and platelet- rich (>16.3%)	Positive linear association with RBC ($p = 0.04$) and a negative linear association with fibrin ($p = 0.01$). Pervious thrombi had higher %RBC (49.8% vs. 33%, $p = 0.006$) and lower %fibrin (17.8% vs. 23.2%, $p = 0.02$). Pervious thrombi were more likely to be RBC-rich (60.5%) than impervious thrombi (31.6%). A trend towards increased platelet content in impervious clots ($p = 0.06$).
Patel (2021)	in vivo	Human	40	2–3 ROIs	High or low perviousness (increase of $>$ 23.75HU or $<$ 23.75HU, respectively)	Histology: H&E	Quantitative (automated): percent F/P, RBC and WBC	Positive correlation with F/P ($r = 0.496$, $p = 0.001$) and negative correlation with RBC ($r = –0.491$, $p = 0.001$). High perviousness thrombi had higher fractions of F/P (55% vs. 40%, $p = 0.042$). Low perviousness thrombi had higher fractions of RBC (53% vs. 38%, $p = 0.040$).
Wei (2021)	in vivo	Human	77	Undefined	Visual	Histology: H&E	Quantitative: percent F/P, RBCs, WBCs	Association with the RBC content ($b = 215$% erythrocytes; 95% CI: 224, 26.2). Pervious thrombi contained higher amounts of RBCs (46%) than impervious samples (34%).
Ye (2021)	in vivo	Human	47	1 ROI	δHU, εHU. Pervious clots, $\delta HU \geq 11$. Impervious clots, $\delta HU < 11$.	Histology: H&E, MSBImmunohistochemistry: von Willebrand factor	Semi-quantitative: component considered rich if greater than the all over median. Quantitative (automated): the proportion of RBC, fibrin and platelets	Pervious clots had significantly lower platelet fractions (19.0% vs. 33.9%, $p = 0.003$) and platelet-rich clots (31.0% vs. 77.8%, $p = 0.002$). Perviousness showed a significantly negative correlation with platelet content [δHU ($r = -0.577$, $p < 0.001$), εHU ($r = -0.573$, $p < 0.001$)].

N for in vitro studies indicates the number of types of thrombus analogs examined. F/P, Fibrin/Platelet; H&E, Hematoxylin and Eosin; HU, Hounsfield Unit; MSB, Martius Scarlet Blue; RBC, Red Blood Cell; ROI, Region of Interest; WBC, White Blood Cell; δHU, absolute perviousness; εHU, relative perviousness.

conglomerations and fewer RBCs (Berndt et al. 2018, Patel et al. 2021). Contrasting to the previous results, Benson et al. (2020) and Wei et al. (2021) found that perviousness was associated with a higher degree of RBC and a lower degree of fibrin. Apart from RBC and fibrin content, Benson et al. (2020) found a trend towards increased platelet content in impervious thrombi. These results are confirmed by Ye et al. (2021) who demonstrated that impervious thrombi had significantly higher platelet fractions (34% vs. 19%, $p = 0.003$). Platelet content was negatively correlated with perviousness (δHU [$r = -0.577$, $p < 0.001$) =], εHU [$r = -0.573$, $p < 0.001$]) (Ye et al., 2021). There are some things to consider with regards to these conflicting findings. First, fibrin proteins attract iodine (contrast agent) (Hertig et al., 2017; McDonald et al., 2014). Second, different methods of in vivo contrast penetration (through the thrombus structure, or gaps between the thrombus and the arterial wall (Wei et al., 2021)) may be contributing to the confusing results. Third, MSB staining allows for the differentiation of platelets from fibrin, while H&E does not (Fitzgerald et al., 2019a). Clot contraction forms tightly-packed RBCs (polyhedrocytes) that may inhibit contrast agent penetration (Cines et al., 2014). This clot contraction is driven by activated platelets (Lam et al., 2011). In line with the Johnson et al. (2019) mechanical data, where clot mechanics differed according to clot contraction, the perviousness of thrombi may

be influenced by the degree of contraction (Ye et al., 2021). Supporting these findings, Gersh et al. (2009) found that permeability of non-contracted clots were not associated with clot histological composition. These experiments should be repeated comparing contracted and non-contracted clots of the same composition. Additionally, Berndt et al. (2018) found a positive correlation between WBC fraction and perviousness, while other studies did not (Benson et al., 2020; Patel et al., 2021). However, the authors warn that this result should be taken with caution due to the small amounts of WBCs present.

2.2.2. *Magnetic resonance imaging*

Table 7 presents the findings for the presence of a **Susceptibility Vessel Sign** (SVS) and thrombus composition. SVS on MRI is mostly determined on T2w gradient recalled echo (GRE) sequences and is defined as a hypointense area or signal loss, which may distort the vessel margins. All studies except one determined an association between thrombus compositions and a SVS. The presence of a SVS is associated with higher amounts of RBCs, and the absence of a SVS with higher amounts of fibrin (Choi et al., 2018; Darcourt et al., 2021; Kim et al., 2015; Liebeskind et al., 2011; Shin et al., 2018). In another study where the gross appearance of the thrombi were qualitatively characterised as white or red–black from photographs, the presence of a SVS also predicted red–black thrombi (Bourcier et al., 2020). In contrast, Horie et al. (2019) did not observe a correlation between RBC concentration and SVS status. The authors postulated that the histology of extracted thrombi may not match that of the in vivo thrombus due to fragmentation and sample damage. However, it should also be noted that this study did not describe the MRI sequence or the definition used for an SVS. Similarly, RBC content, quantified with haemoglobin enzyme-linked immunosorbent assays and colouration with formic acid, did not differ between thrombi with the presence or absence of SVS (Di Meglio et al., 2020). Here, the authors suggest that semi-quantitative analysis of thrombus composition on histology may be a source of bias as it evaluates only a part of the thrombus. Additionally, they attribute the lack of standardisation of MRI sequences as another explanation for the contrasting findings.

A two-layered SVS is an inhomogeneous SVS that contains a lower intensity core surrounded by a higher intensity signal (Yamamoto et al., 2015). RBC concentration did differ between thrombi with or without a two-layered SVS (Di Meglio et al., 2020). Bourcier et al. (2020) did not observe a similar relationship between red–black thrombus and a two layered-SVS. Di Meglio et al. (2020) recommend two layered-SVS as a more reliable marker of RBC-rich thrombus based on their quantitative assay analysis. The authors also investigated the proportion of WBCs in thrombi, but these percentages were not significantly related to SVS.

Other in vitro studies quantified the **signal intensities** from various MRI sequences and associated the findings against thrombus composition using either histology, spectroscopy or known component ratios (Table 8). Fujimoto and colleagues were able to distinguish RBC-rich and fibrin-rich thrombus analogs using mean thrombus signal intensities in both an in vitro and a swine model. Bourcier et al. (2019) found a significant negative correlation between the T2* relaxation time and the RBC concentration of 7 different thrombus analogs. Another study used R2* quantitative susceptibility mapping and proton density fat fraction maps to characterise thrombus analogs with varying hematocrit, in addition to calcific and lipidic components (Christiansen

Table 7
Studies that assessed the association between thrombus composition and the presence of a susceptibility weighted vessel sign on magnetic resonance images.

Study	Type	Species	n	MRI Sequence	Imaging Sign	SVS Method	Compositional Method	Compositional Analysis	Results
Liebeskind (2011)	in vivo	Human	32	GRE	SVS	Visual inspection	Histology: H&E	Quantitative: proportion of fibrin, RBCs and WBCs. Qualitative: RBC-rich, fibrin-rich, mixed (undefined).	RBC content was greater with SVS (42% vs. 23%, $p = 0.011$). SVS was more common in RBC-rich and mixed thrombi compared to fibrin-rich thrombi (100% vs. 63% vs. 25%, $p = 0.002$).
Kim (2015)	in vivo	Human	37	GRE	SVS	Visual inspection	Histology: H&E Immunohistochemistry: CD61	Quantitative: percent RBC, fibrin, platelets and WBCs	RBC was greater with SVS (48% vs. 1.9%, $p < 0.001$). Fibrin and platelets were greater without SVS (26.4% vs. 57%, $p < 0.001$ and 22.6% vs. 36.9%, $p = 0.011$).
Choi (2018)	in vivo	Human	52	GRE	SVS	Visual inspection	Histology: H&E, MSB	Quantitative: percent RBC, F/P and WBCs. Semi-quantitative: RBC tertiles.	Higher RBC tertiles were more commonly associated with SVS (91.7% vs. 66.7% vs. 50%, $p = 0.022$).
Shin (2018)	in vivo	Human	37	GRE	SVS	Visual inspection	Histology: H&E	Quantitative: percent RBC, F/P and WBCs	RBCs was higher in thrombi with a SVS (39% vs. 16% $p = 0.001$).
Horie (2018)	in vivo	Human	65	Undefined	SVS	Undefined	Histology: H&E	Quantitative: percent RBC and fibrin	The presence of a SVS was not correlated with the percentage of RBCs.
Bourcier (2020)	in vivo	Human	139	GRE	SVS and TL-SVS	Visual inspection	Photographs (visual)	Qualitative: white or red–black	SVS was an independent predictor for red thrombus (odd ratio 8.31, 95% CI 2.30 to 32, p value < 0.001).
Di Meglio (2020)	in vivo	Human	84	GRE or SWI	SVS and TL-SVS	Visual inspection	ELISA, colouration with formic acid, flow cytometry	Quantitative: total HG content	TLSVS thrombi had a higher HG content (278 [221–331] μg/mg) than those without TLSVS (196 [139–301] μg/mg), $p = 0.01$.
Darcourt (2021)	in vivo	Human	102	T2*GRE	SVS	Visual inspection	Histology: H&E	Quantitative: percent RBC, F/P	SVS thrombi had significantly higher amounts of RBCs (42.4 ± 25.7%) and lower amounts of F/P (57.6 ± 25.7%).

GRE, Gradient-Echo Recalled; ELISA, Enzyme-Linked Immunosorbent Assay; HG, Haemoglobin; H&E, Hematoxylin and Eosin staining; MSB, Martius Scarlet Blue staining; RBC, Red Blood Cell; SVS, Susceptibility Vessel Sign; SWI, Susceptibility Weighted Imaging; WBC, White Blood Cell.

Table 8
Studies that assessed the association between thrombus composition and signal intensity on magnetic resonance images.

Study	Type	Species	n	MRI Sequence	Magnet	Imaging Method	Compositional Method	Compositional Analysis	Results
Fujimoto (2013)	in vitro (static)	Swine	2	GRE, FLAIR and T2W	3 T	Mean signal intensity	Known from thrombus analog protocols	Qualitative: RBC-rich and fibrin-rich	FLAIR and T2W were able to identify the RBC from other components.
Bourcier (2019)	in vitro (static and dynamic[a])	Ovine	7	GRE	1.5 T	1 ROI, mean T2*RT	Histology: H&E	Quantitative: percent F/P, RBC and WBC	A strong negative correlation was found between T2*RT and RBC content ($r = -0.834$, $p < 0.001$).
Christiansen (2019)	in vitro (static)	Porcine	8	3D multi-echo GRE	3 T	1 ROI, mean and SD R_{2*}, QSM and FF maps	Volumetric ratios	Semi-quantitative: 10%, 20%, 30%, 40%, 50%, and 60% RBC, sample containing lipid or calcium carbonate	R2* and QSM maps can be used to determine thrombus RBC composition. QSM and FF maps can distinguish between lipid and calcification.
Bretzner (2020)	in vitro (static)	Ovine	12	3D multi-echo GRE	7 T	R2* relaxometry	Absorption spectrometry (iron concentrations) and histology: MY and SR (RBC)	Quantitative: RBC counting	R2* values were positively correlated with RBC content ($r = 0.80$, $p = 0.02$) and iron content ($r = 0.79$, $p = 0.02$).
Janot (2020)	in vitro (static and dynamic[a])	Ovine	9	GRE, SWI, FLAIR	3 T	1 ROI, mean signal intensity	Histology: H&E	Quantitative: percent RBC. Semi-quantitative: no RBCs, >50% RBCs, 50% RBCs and < 50% RBCs.	RBC content is inversely related to the signal intensity from SWI and GRE sequences for four different regression models: $r = 0.981$; 0.986; 0.994, and 0.971.

N for in vitro studies indicates the number of types of thrombus analogs examined. FF, proton density Fat Fraction; FLAIR, Fluid-Attenuated Inversion Recovery; F/P, Fibrin/Platelet; H&E, Hematoxylin and Eosin; MSB, Martius Scarlet Blue; MY, Martius Yellow; QSM, Quantitative Susceptibility Mapping; RBC, Red Blood Cell; ROI, Region of Interest; SD, standard deviation; SR, Scarlet Red; T2W, T2-Weighted; WBC, White Blood Cell.
[a] Modified Chandler Loop technique.

et al., 2019). With these maps, thrombi of varying hematocrit, as well as lipid and calcium areas, could be distinguished from each other. Bretzner et al. (2020) used R2* relaxometry of thrombus analogs to determine the correlation between texture maps and thrombus composition and analysed the spatial distribution of the composition. R2* values were positively correlated to the RBC concentration and iron concentration. These results conducted on a 7 T MRI complement those by Bourcier et al. (2019) and Christiansen et al. (2019). The signal intensity ratios of susceptibility-weighted imaging and T2-weighted gradient-echo negatively correlated with RBC concentration, but were unable to distinguish RBC concentration > 54% and < 23% (Janot et al., 2020). RBC concentration could be quantified by combining T2-weighted gradient-echo, susceptibility-weighted imaging and fluid-attenuated inversion recovery sequences.

2.2.3. Digital subtraction angiography

Only one study compared thrombus imaging characteristics from DSA images to thrombus composition (Mönch et al., 2019). The proximal end of the thrombus was categorised as cut off, tapered, meniscus, or tram-track in 144 patients. The ratios of fibrin/platelets, RBCs and WBCs from H&E-stained sections were compared between the groups. However, proximal thrombus appearance could not be associated with thrombus composition. The authors suggest that future studies with larger patient numbers might find associations between thrombus appearance and histological composition.

3. Discussion

3.1. Is it clinically relevant to image thrombus composition?

Thrombus composition has proved to be associated with EVT procedure metrics, recanalization, and clinical outcomes. RBC-rich thrombi have been associated with shorter procedural duration, a lower number of device passes (Maekawa et al., 2018; Sporns et al., 2017), and successful recanalization (Froehler et al., 2013; Hashimoto et al., 2016; Jolugbo and Ariëns, 2021; Mokin et al., 2015; Shin et al., 2018). On the other hand, RBC-rich thrombi are more prone to migration than fibrin-rich thrombi (Sporns et al., 2020). Further, in per-pass analyses of thrombus composition, it was demonstrated that the RBC content of fragments retrieved in the initial passes are higher than those retrieved in the later passes (Boodt et al., 2021; Duffy et al., 2019). This is in line with previous studies demonstrating that fibrin-rich thrombi require a higher number of attempts to retrieve than RBC-rich thrombi (Yuki et al., 2012). Finally, hard thrombus analogs displayed an increased number of visible embolic particles compared with soft clot analogs that were prone to release much smaller embolic particles during in vitro thrombectomy (Chueh et al., 2013). Collectively, these findings **support the clinical need** to determine the thrombus composition prior to EVT.

3.2. Is thrombus composition related to mechanical properties?

Our review provides evidence that thrombus mechanics are related to thrombus composition under a variety of loading conditions. RBC-rich thrombi are less stiff than fibrin-rich thrombi. This explains why fibrin-rich thrombi are more difficult to retrieve (Sporns et al., 2017; Yuki et al., 2012). The reduced stiffness of RBC-rich thrombi allows stent struts to penetrate deeper into the thrombus matrix (Weafer et al., 2019) and enhance the interaction between the thrombus and the device. In contrast, the increased stiffness of fibrin-rich samples does not allow the stent struts to immediately indent into the clot leading to failed retrieval attempts. Most studies had not considered the viscoelastic behaviour of the thrombi and how this may affect stent strut indentation. Weafer et al. (2019) determined that an embedding time is more relevant for fibrin-rich thrombi and identified stretching of the fibrin networks as the primary mechanism of additional embedding of the stent strut. These results complement that of a previous study that found that the push and fluff technique, combined with 5 mins of embedding time, versus standard unsheathing and no embedding time, maximized the integration of

the Trevo stent-retriever with hard inelastic clots (Van Der Marel et al. 2016).

Fibrin-rich thrombi also have higher coefficients of friction than RBC-rich thrombi (Gunning et al. 2018) The samples were tested on an artificial surface, and the results were validated on a bovine aortic surface. This test describes the friction between fresh thrombi and a healthy vessel wall. However, friction forces also exist between EVT devices and the thrombus, which have yet to be determined. Furthermore, ex vivo thrombi have exhibited surface endothelialisation and an organised structure (Boeckh-Behrens et al., 2016; Niesten et al., 2014) that may affect the adhesion properties between the thrombus and the vessel wall.

Mechanical characterisation studies suggest that fibrin-rich clots are more resistant to fragmentation compared with clots that have a higher RBC content. The clinical evidence of the relation between clot composition and thrombus fragmentation is not as conclusive. Ye et al. (2020) and Kaesmacher et al. (2017) observed trends towards higher RBC fractions and periprocedural thrombus fragmentation, however, the results were not statistically significant in multivariable analysis. Sporns et al. (2017) found the opposite association with fibrin-rich thrombi causing more periprocedural secondary embolisms. An in vitro study by Chueh et al. (2013) examined embolic particles with respect to size. Here, hard (bovine) and soft (human) thrombus analogs were prone to release larger and smaller emboli, respectively. However, the results are not analysed according to composition. With clinical imaging, it may be difficult to capture embolic particles smaller than the resolution of the imaging modality. Kaesmacher et al. (2017) did find an association between WBCs and thrombus fragmentation. The studies of Fereidoonnezhad et al. (2021) and Liu et al. (2021) suggest that clot contraction also affects the fracture properties of thrombi. Further, the RBC content of fragments retrieved in the initial passes is higher than those retrieved in the later passes (Boodt et al., 2021; Duffy et al., 2019), suggested that thrombi will fragment at the interface of differential compositions. These associations (WBCs, clot contraction and interfaces) have not been examined in mechanical characterisation studies yet.

The representativeness of thrombus analogs for mechanical characterization of thrombi is a matter of debate. A common conclusion is that thrombus analogs span the range of stiffness displayed by human samples (Chueh et al., 2011; Liu et al., 2020a) or that they match high-strain (but not low-strain) stiffness (Johnson et al., 2019). Considering the wide degree of variability exhibited by human tissue (Chueh et al., 2011; Liu et al., 2020b), this conclusion is not surprising. Findings from recent histopathological analysis of EVT retrieved thrombi must be used to develop more realistic thrombus analogs (Staessens et al., 2020). In vitro studies should also strive to include a range of analogs with varying compositions to represent this diversity (Johnson et al., 2017; Weafer et al., 2019). However, in vitro studies in the current review include as little as two types of thrombi (Janis et al., 2001; Machi et al., 2017). Moreover, the volumetric ratio of RBC in the thrombus analogs does not produce thrombi with equivalent RBC content (Duffy et al., 2017). Another issue arises from the fact that human thrombi are formed under dynamic conditions of physiological pressure and flow, and this produces thrombi with heterogeneous compositions. Almost all thrombus analogs utilised in the studies in this review were formed under static conditions. Those formed under dynamic conditions consisted of a modified Chandler Loop setup or spun during maturation in a centrifuge. Additionally, a further set of loading is applied to thrombi during the EVT retrieval. It has been shown that repeated deformations can alter the structure of a thrombus (Münster et al., 2013). Mechanisms for such permanent effects include protein unfolding, fibre deformations (buckling, bending and reorientation), densification of the fibrin network and the expulsion of fluid from the system (Brown, 2009; Kim et al., 2014; Liang et al., 2017; Piechocka et al., 2010). This would also explain the difficulty in the retrieval of fibrin-rich samples and could also indicate that with each pass, the sample may be increasingly difficult to retrieve. Only two studies applied a pre-load to thrombus analogs prior to indentation (Weafer et al., 2019) or unconfined compression (Chueh et al., 2011). However, these pre-loads were likely too small to replicate the supraphysiological loading experienced by EVT specimens during retrieval. This may also explain the differences that occur in the low-strain behaviour of thrombus analogs compared with human thrombi.

3.3. *Is it useful and feasible to assess compositional and mechanical properties quantitatively with imaging?*

Clot signs such as the HAS and the SVS can successfully identify RBC-rich samples. However, the highly heterogeneous nature of AIS thrombi will limit the use of these categorical analyses (Jolugbo and Ariëns, 2021). In this regard, efforts should be made to work towards quantified measures such as density or signal intensity for future studies.

DSA measurements are qualitative and cannot be reliably done before the treatment technique or device is chosen, so it will likely not help increase EVT effectiveness. MRI may be a useful modality for thrombus characterisation. However, the time required to complete an MRI scan is longer than that of a CT scan. It has also been shown that the diagnostic accuracy of the SVS measured on different MRI scanners using the same sequences can vary significantly (Bourcier et al., 2017). While quantitative signal intensity mapping has been recommended, it is not currently used in radiological imaging stroke protocols (Janot et al., 2020). Some of these imaging protocols are readily transferrable to the clinic (Christiansen et al., 2019), while others are not (Bretzner et al., 2020). In terms of the three primary modalities discussed here, computed tomography is already performed before thrombectomy in most centres, as it is the gold standard in acute stroke diagnosis. Therefore, CT holds the most promise for introducing a pretreatment thrombus characterisation step into the stroke management workflow.

CT can be performed with or without contrast enhancement. With NCCT it is possible to quantitatively assess the density values. The majority of studies found a positive correlation between RBC concentration and thrombus density. This quantified thrombus density and RBC percentages could be useful for predicting exact mechanics. However, the clinical applicability of quantified thrombus density depends on the coefficient and significance of the relationship, which is variable (Table 5). This may be attributed to the variation in CT acquisition protocols and characteristics such as slice thickness, a parameter known to affect CT density outcomes (Tolhuisen et al., 2017). Moreover, in multi-centre studies, the image acquisition protocols can vary and the resulting scan parameters are often not reported. In this regard, it is difficult to directly compare studies. More standardized subsequent or retrospective studies with larger sample sizes should be performed, so that results can be directly compared and definitive conclusions can be drawn.

With CTA it is possible to determine the thrombus perviousness, a proxy for thrombus permeability. While there are some contrasting results so far on the association of thrombus perviousness with thrombus composition, perviousness is a recently developed radiological imaging thrombus characteristic so a small number of studies are currently conducted on this association. Furthermore, with in vivo studies, it is difficult to know whether an increase in density is caused by the diffusion of the contrast agent through the thrombus matrix or whether a gap exists between the thrombus and the arterial wall, which may create a false increase in density. Some recent results have suggested that perviousness is associated with platelet-driven clot contraction since trends are evident between thrombus perviousness and platelet content (Benson et al., 2020; Ye et al., 2021). This hypothesis may be best resolved by conducting in vitro perviousness or permeability tests in a controlled environment similar to previous work by Gersh et al. (2009).

Thrombus **stiffness** is largely driven by the fibrin network. There is currently no clinical means of characterising the fibrin network in vivo. Given this, if one assumes that the fibrin content and the RBC content are largely the opposite of one another, then quantifying density on NCCT would inversely reflect the general stiffness of the thrombus. There are

conflicting results in the literature stating that either fibrin-rich or RBC-rich thrombi respond better to contact aspiration or stent retrieval (Bourcier et al., 2018; Madjidyar et al., 2020; Mohammaden et al., 2020). Knowledge of the **device-tissue interaction** should shed some light on this topic. There are currently two EVT approaches (a stent retriever or aspiration catheter) and three methods of deploying a stent retriever: the standard unsheathing, the puff and fluff technique (Haussen et al., 2015) and the use of an embedding time (Weafer et al., 2019). As demonstrated by Weafer et al. (2019), the indentation of stent strut into the thrombus matrix is determined by the stretching of fibrin fibres in thrombi with lower RBC content and the rupture of fibres are higher RBC content. Similar studies are required that characterise the deformability and viscoelasticity of thrombus with differing compositions upon contact with an aspiration catheter tip. An embedding time is most relevant for fibrin-rich thrombi in the case of stent retrievers. This may also be the case for aspiration catheters. Alternatively, RBCs have exhibited high deformability (Dobbe et al., 2002) that may be relevant for shape change upon introduction into the smaller catheter. Different studies suggest that either RBC-rich samples (Maegerlein et al., 2018; Yuki et al., 2012) or fibrin-rich samples (Kaesmacher et al., 2017; Sporns et al., 2017) are more likely to **fragment**. Moreover, the differential composition of thrombi retrieved in sequential passes indicates that thrombi may fragment at the boundary between fibrin-rich and RBC-rich portions (Duffy et al., 2019). A further complication includes the choice of EVT device: either an aspiration catheter or a stent-retriever. Aspiration catheters only make contact with the proximal segment of the thrombus and do not contact the distal portion to provide any support against fragmentation (Mohammaden et al., 2020). However, it was also found that the embedding of stent struts into RBC-rich samples increased the fibrin-rupture observed (Weafer et al., 2019), this may, in turn, increase the risk of distal embolization with the use of stent retrievers. The key to understanding this fragmentation is the fracture properties of the fibrin network. Tutwiler et al. (2020) have previously examined the fracture behaviour of pure fibrin networks. However, the introduction of other cellular components is known to alter this network architecture. A dense fibrin network is associated with the platelet content (Staessens et al., 2020), while higher amounts of RBCs results in a thinner network of thicker fibres (Gersh et al., 2009; Staessens et al., 2020). Therefore, to understand the risk of thrombus fragmentation we need to examine the fracture properties of fibrin networks with the (heterogeneous) inclusion of the relevant cellular (and molecular) components and characterise the fibrin network architecture by examining the fibre density, diameter, orientation, pore size, branching and cross-linking.

3.4. *What else should be considered besides thrombus composition?*

While this review highlights the intimate link between thrombus composition and mechanics, there is quite some variation in the findings. There are some factors besides thrombus composition that can play a role in the observed mechanical characteristics.

Samples that underwent **platelet-driven clot contraction** were found to be stiffer in compression and shear (Johnson et al., 2019; Liang et al., 2017). Preliminary data also suggest that contracted clots have different failure properties than non-contracted clots (Fereidoonnezhad et al., 2021). Importantly, this change in clot mechanics was observed without an appreciable difference in clot histological composition (Johnson et al., 2019). This is relevant as stroke patients can exhibit impaired clot contraction (Tutwiler et al., 2017). The effect of clot contraction on admission imaging characteristics has not been examined yet. As mentioned previously, it is hypothesised that perviousness reflects the degree of clot contraction, but this hypothesis remains to be tested.

Bridging intravenous recombinant tissue plasminogen activator (IV-rtPA) with EVT is the current standard of care for large vessel occlusion patients in patients eligible to receive IV-rtPA (Powers et al., 2019). Ex vivo and in vitro analyses suggest that while IV-rtPA administration reduces the clot size or mass (Dwivedi et al., 2021; Rossi et al., 2021), it does not alter clot composition (Kaesmacher et al., 2017; Patel et al., 2021; Rossi et al., 2021). To the authors' knowledge, only one study has directly examined the effect of IV-rtPA administration on clot mechanical properties in an in vitro setup (Dwivedi et al., 2021). Despite the unchanged clot composition after IV-rtPA, Dwivedi et al. (2021) report that both clot stiffness and viscoelastic behaviour are affected by IV-rtPA exposure. The question remains whether alterations in thrombus mechanics caused by IV-rtPA can be identified in admission imaging.

In summary, knowledge of the thrombus composition prior to retrieval will identify which methods are most suitable on a case-by-case basis. The three primary properties of thrombi that will govern its response to EVT treatment include stiffness (the resistance to deform in response to a force), friction (the resistance of motion between the thrombus and the vessel wall or the device) and fracture (the tendency to fragment). Currently, it is possible to identify RBC-rich or fibrin-rich thrombi using vessel signs on CT and MRI scans. To reliably predict thrombus stiffness using admission NCCT, quantified thrombus density values must be associated with quantified RBC content in a standardised manner. However, the focus of radiological imaging may need to shift from RBC quantification to the characterisation of the fibrin network architecture to predict device-tissue interaction and the risk of thrombus fragmentation. In addition to clot composition, perviousness may be able to determine the degree of clot contraction.

CRediT authorship contribution statement

Rachel Cahalane: Conceptualization, Methodology, Investigation, Writing – original draft, Writing – review & editing, Visualization. **Nikki Boodt:** Conceptualization, Methodology, Investigation, Writing – original draft, Writing – review & editing. **Ali Cagdas Akyildiz:** Writing – review & editing. **Jo-anne Giezen:** Writing – original draft. **Manouk Mondeel:** Writing – original draft. **Aad van der Lugt:** Conceptualization, Writing – review & editing, Supervision, Funding acquisition. **Henk Marquering:** Conceptualization, Methodology, Writing – review & editing, Supervision. **rank Gijsen:** Conceptualization, Writing – review & editing, Supervision, Funding acquisition.

Declaration of Competing Interest

The authors declare that they have no known competing financial interests or personal relationships that could have appeared to influence the work reported in this paper.

Acknowledgements

This study is funded by the Erasmus MC, University Medical Center Rotterdam under the Augmented Human Initiative and the European Union's Horizon 2020 research and innovation program under grant agreement No 777072.

Appendix A. Supplementary material

Supplementary data to this article can be found online at https://doi.org/10.1016/j.jbiomech.2021.110816.

References

Alkarithi, G., Duval, C., Shi, Y., Macrae, F.L., Ariëns, R.A.S., 2021. Thrombus Structural Composition in Cardiovascular Disease. Arterioscler. Thromb. Vasc. Biol. 2370–2383 https://doi.org/10.1161/atvbaha.120.315754.

Almekhlafi, M.A., Hu, W.Y., Hill, M.D., Auer, R.N., 2008. Calcification and endothelialization of thrombi in acute stroke. Ann. Neurol. 64, 344–347. https://doi.org/10.1002/ana.21404.

Benson, John Charles, Fitzgerald, S.T., Kadirvel, R., Johnson, C., Dai, D., Karen, D., Kallmes, D.F., Brinjikji, W., 2020. Clot permeability and histopathology: is a clot's perviousness on CT imaging correlated with its histologic composition?

J. Neurointerv. Surg. 12, 38. https://doi.org/10.1136/neurintsurg-2019-014979. LP – 42.
Berkhemer, O.A., Fransen, P.S.S., Beumer, D., Van Den Berg, L.A., Lingsma, H.F., Yoo, A. J., Schonewille, W.J., Vos, J.A., Nederkoorn, P.J., Wermer, M.J.H., Van Walderveen, M.A.A., Staals, J., Hofmeijer, J., Van Oostayen, J.A., Lycklama Nijeholt, G.J., Boiten, J., Brouwer, P.A., Emmer, B.J., De Bruijn, S.F., Van Dijk, L.C., Kappelle, L.J., Lo, R.H., Van Dijk, E.J., De Vries, J., De Kort, P.L.M., Van Rooij, W.J. J., Van Den Berg, J.S.P., Van Hasselt, B.A.A.M., Aerden, L.A.M., Dallinga, R.J., Visser, M.C., Bot, J.C.J., Vroomen, P.C., Eshghi, O., Schreuder, T.H.C.M.L., Heijboer, R.J.J., Keizer, K., Tielbeek, A.V., Den Hertog, H.M., Gerrits, D.G., Van Den Berg-Vos, R.M., Karas, G.B., Steyerberg, E.W., Flach, H.Z., Marquering, H.A., Sprengers, M.E.S., Jenniskens, S.F.M., Beenen, L.F.M., Van Den Berg, R., Koudstaal, P.J., Van Zwam, W.H., Roos, Y.B.W.E.M., Van Der Lugt, A., Van Oostenbrugge, R.J., Majoie, C.B.L.M., Dippel, D.W.J., 2015. A randomized trial of intraarterial treatment for acute ischemic stroke. N. Engl. J. Med. 372, 11–20. https://doi.org/10.1056/NEJMoa1411587.
Berndt, M., Friedrich, B., Maegerlein, C., Moench, S., Hedderich, D., Lehm, M., Zimmer, C., Straeter, A., Poppert, H., Wunderlich, S., Schirmer, L., Oberdieck, P., Kaesmacher, J., Boeckh Behrens, T., 2018. Thrombus permeability in admission computed tomographic imaging indicates stroke pathogenesis based on thrombus histology. Stroke 49, 2674–2682. https://doi.org/10.1161/STROKEAHA.118.021873.
Boeckh-Behrens, T., Schubert, M., Förschler, A., Prothmann, S., Kreiser, K., Zimmer, C., Riegger, J., Bauer, J., Neff, F., Kehl, V., Pelisek, J., Schirmer, L., Mehr, M., Poppert, H., 2016. The Impact of Histological Clot Composition in Embolic Stroke. Clin. Neuroradiol. 26, 189–197. https://doi.org/10.1007/s00062-014-0347-x.
Boodt, N., Snouckaert van Schauburg, P., Hund, H., Fereidoonnezhad, B., McGarry, P., Akyildiz, A., van Es, A., De Meyer, S., Dippel, D., Lingsma, H., van Beusekom, H., van der Lugt, A., Gijsen, F., 2021. Mechanical Characterization of Thrombi Retrieved with Endovascular Thrombectomy in Patients with Acute Ischemic Stroke. Stroke. https://doi.org/10.1161/STROKEAHA.120.033527.
Borggrefe, J., Kottlors, J., Mirza, M., Neuhaus, V.-F., Abdullayev, N., Maus, V., Kabbasch, C., Maintz, D., Mpotsaris, A., 2018. Differentiation of Clot Composition Using Conventional and Dual-Energy Computed Tomography. Clin. Neuroradiol. 28, 515–522. https://doi.org/10.1007/s00062-017-0599-3.
Pautre Bourcier, R., Mirza, M., Castets, C., Darcourt, J., Labreuche, J., Detraz, L., Desal, H., Serfaty, J.M., Toquet, C., Bourcier, R., 2019. MRI quantitative T2* mapping to predict dominant composition of in vitro thrombus. Am. J. Neuroradiol. 40, 59–64. https://doi.org/10.3174/ajnr.A5938.
Bourcier, R., Détraz, L., Serfaty, J.M., Delasalle, B.G., Mirza, M., Derraz, I., Toulgoat, F., Naggara, O., Toquet, C., Desal, H., 2017. MRI Interscanner Agreement of the Association between the Susceptibility Vessel Sign and Histologic Composition of Thrombi. J. Neuroimaging 27, 577–582. https://doi.org/10.1111/jon.12464.
Bourcier, R., Duchmann, Z., Sgreccia, A., Desal, H., Carità, G., Desilles, J.P., Lapergue, B., Consoli, A., 2020. Diagnostic Performances of the Susceptibility Vessel Sign on MRI for the Prediction of Macroscopic Thrombi Features in Acute Ischemic Stroke. J. Stroke Cerebrovasc. Dis. 29 https://doi.org/10.1016/j.jstrokecerebrovasdis.2020.105245.
Bourcier, R., Mazighi, M., Labreuche, J., Fahed, R., Blanc, R., Gory, B., Duhamel, A., Marnat, G., Saleme, S., Costalat, V., Bracard, S., Desal, H., Consoli, A., Piotin, M., Lapergue, B., 2018. Erratum: Susceptibility vessel sign in the aster trial: Higher recanalization rate and more favourable clinical outcome after first line stent retriever compared to contact aspiration (Journal of Stroke, (2018) 20(2), (268-276), 10.5853/jos.2018.00192). J. Stroke 20, 416. https://doi.org/10.5853/jos.2018.00192.e1.
Bretzner, M., Lopes, R., McCarthy, R., Corseaux, D., Auger, F., Gunning, G., Beauval, N., Bongiovanni, A., Tardivel, M., Cordonnier, C., Pruvo, J.P., Susen, S., Leclerc, X., Kuchcinski, G., 2020. Texture parameters of R2* maps are correlated with iron concentration and red blood cells count in clot analogs: A 7-T micro-MRI study. J. Neuroradiol. 47, 306–311. https://doi.org/10.1016/j.neurad.2019.10.004.
Brinjikji, W., Duffy, S., Burrows, A., Hacke, W., Liebeskind, D., Majoie, C.B.L.M., Dippel, D.W.J., Siddiqui, A.H., Khatri, P., Baxter, B., Nogeuira, R., Gounis, M., Jovin, T., Kallmes, D.F., 2017a. Correlation of imaging and histopathology of thrombi in acute ischemic stroke with etiology and outcome: A systematic review. J. Neurointerv. Surg. 9, 529–534. https://doi.org/10.1136/neurintsurg-2016-012391.
Brinjikji, W., Michalak, G., Kadirvel, R., Dai, D., Gilvarry, M., Duffy, S., Kallmes, D.F., McCollough, C., Leng, S., 2017b. Utility of single-energy and dual-energy computed tomography in clot characterization: An in-vitro study. Interv. Neuroradiol. 23, 279–284. https://doi.org/10.1177/1591019917694479.
Brouwer, P.A., Brinjikji, W., De Meyer, S.F., 2018. Clot Pathophysiology: Why Is It Clinically Important? Neuroimaging Clin. N. Am. 28, 611–623. https://doi.org/10.1016/j.nic.2018.06.005.
Brown, A.E.X., 2009. Multiscale Mechanics of Fibrin Unfolding and Loss of Water. Science (80-.) 325, 741–744. https://doi.org/10.1126/science.1172484.
Campbell, B.C.V., Mitchell, P.J., Kleinig, T.J., Dewey, H.M., Churilov, L., Yassi, N., Yan, B., Dowling, R.J., Parsons, M.W., Oxley, T.J., Wu, T.Y., Brooks, M., Simpson, M. A., Miteff, F., Levi, C.R., Krause, M., Harrington, T.J., Faulder, K.C., Steinfort, B.S., Priglinger, M., Ang, T., Scroop, R., Barber, P.A., McGuinness, B., Wijeratne, T., Phan, T.G., Chong, W., Chandra, R.V., Bladin, C.F., Badve, M., Rice, H., De Villiers, L., Ma, H., Desmond, P.M., Donnan, G.A., Davis, S.M., 2015. Endovascular therapy for ischemic stroke with perfusion-imaging selection. N. Engl. J. Med. 372, 1009–1018. https://doi.org/10.1056/NEJMoa1414792.
Carr, C., 1995. Fibrin structure and concentration alter clot elastic modulus but do not alter platelet mediated force development. Blood Coagul. Fibrinolysis. https://doi.org/10.1097/00001721-199502000-00013.
Choi, M.H., Park, G.H., Lee, J.S., Lee, S.E., Lee, S.J., Kim, J.H., Hong, J.M., 2018. Erythrocyte fraction within retrieved thrombi contributes to thrombolytic response in acute ischemic stroke. Stroke 49, 652–659. https://doi.org/10.1161/STROKEAHA.117.019138.
Christiansen, S.D., Liu, J., Boffa, M.B., Drangova, M., 2019. Simultaneous R2* and quantitative susceptibility mapping measurement enables differentiation of thrombus hematocrit and age: An in vitro study at 3T. J. Neurointerv. Surg. 11, 1155–1161. https://doi.org/10.1136/neurintsurg-2019-014802.
Chueh, J.Y., Kühn, A.L., Puri, A.S., Wilson, S.D., Wakhloo, A.K., Gounis, M.J., 2013. Reduction in distal emboli with proximal flow control during mechanical thrombectomy: A quantitative in vitro study. Stroke 44, 1396–1401. https://doi.org/10.1161/STROKEAHA.111.670463.
Chueh, J.Y., Wakhloo, A.K., Hendricks, G.H., Silva, C.F., Weaver, J.P., Gounis, M.J., 2011. Mechanical characterization of thromboemboli in acute ischemic stroke and laboratory embolus analogs. Am. J. Neuroradiol. 32, 1237–1244. https://doi.org/10.3174/ajnr.A2485.
Cines, D.B., Lebedeva, T., Nagaswami, C., Hayes, V., Massefski, W., Litvinov, R.I., Rauova, L., Lowery, T.J., Weisel, J.W., 2014. Clot contraction: Compression of erythrocytes into tightly packed polyhedra and redistribution of platelets and fibrin. Blood 123, 1596–1603. https://doi.org/10.1182/blood-2013-08-523860.
Darcourt, J., Garcia, C., Phuong, D.M., Michelozzi, C., Bellanger, G., Adam, G., Roques, M., Januel, A.C., Tall, P., Albucher, J.F., Olivot, J.M., Bonneville, F., Payrastre, B., Cognard, C., 2021. Absence of susceptibility vessel sign is associated with aspiration-resistant fibrin/platelet-rich thrombi. Int. J. Stroke. https://doi.org/10.1177/1747493020986626, 174749302098662.
Dempfle, C.E., Kälsch, T., Elmas, E., Suvajac, N., Lücke, T., Münch, E., Borggrefe, M., 2008. Impact of fibrinogen concentration in severely ill patients on mechanical properties of whole blood clots. Blood Coagul. Fibrinolysis 19, 765–770. https://doi.org/10.1097/MBC.0b013e32830f1b68.
Di Meglio, L., Derraz, I., Solonomenjanahary, M., Daly, D., Chodraui Filho, S., Ben Maacha, M., Labreuche, J., Desal, H., Consoli, A., Lapergue, B., Blanc, R., Piotin, M., Mazighi, M., Ho-Tin-Noé, B., Desilles, J.P., Bourcier, R., Redjem, H., Smajda, S., Ciccio, G., Fahed, R., Escalard, S., Hamdani, M., Sabben, C., Obadia, M., Deschildre, C., Hebert, S., Rodesch, G., Di Maria, F., Coskun, O., Lopez, D., Detraz, L., Roy, M., Clavier, D., Marnat, G., Gariel, F., Lucas, L., Sibon, I., Eugene, F., Vannier, S., Ferre, J.C., LeBras, A., Raoult, H., Paya, C., Gauvrit, J.Y., Richard, S., Gory, B., Delvoye, F., Maier, B., 2020. Two-layered susceptibility vessel sign is associated with biochemically quantified thrombus red blood cell content. Eur. J. Neurol. 27, 1264–1271. https://doi.org/10.1111/ene.14241.
Ding, Y.-H., Abbasi, M., Michalak, G., Leng, S., Dai, D., Fitzgerald, S., Kadirvel, R., Kallmes, D.F., Brinjikji, W., 2020. Characterization of thrombus composition with multimodality CT-based imaging: an in-vitro study. J. Neurointerv. Surg. neurintsurg-2020-016799. https://doi.org/10.1136/neurintsurg-2020-016799.
Dobbe, J.G.G., Hardeman, M.R., Streekstra, G.J., Strackee, J., Ince, C., Grimbergen, C.A., 2002. Analyzing red blood cell-deformability distributions. Blood Cells. Mol. Dis. 28, 373–384. https://doi.org/10.1006/bcmd.2002.0528.
Duffy, S., Farrell, M., McArdle, K., Thornton, J., Vale, D., Rainsford, E., Morris, L., Liebeskind, D.S., MacCarthy, E., Gilvarry, M., 2017. Novel methodology to replicate clot analogs with diverse composition in acute ischemic stroke. J. Neurointerv. Surg. 9, 486–491. https://doi.org/10.1136/neurintsurg-2016-012308.
Duffy, S., Mccarthy, R., Farrell, M., Thomas, S., Brennan, P., Power, S., O'Hare, A., Morris, L., Rainsford, E., Maccarthy, E., Thornton, J., Gilvarry, M., 2019. Per-Pass Analysis of Thrombus Composition in Patients With Acute Ischemic Stroke Undergoing Mechanical Thrombectomy. Stroke 50, 1156–1163. https://doi.org/10.1161/STROKEAHA.118.023419.
Dutra, B.G., Tolhuisen, M.L., Alves, H.C.B.R., Treurniet, K.M., Kappelhof, M., Yoo, A.J., Jansen, I.G.H., Dippel, D.W.J., Van Zwam, W.H., Van Oostenbrugge, R.J., Da Rocha, A.J., Lingsma, H.F., Van Der Lugt, A., Roos, Y.B.W.E.M., Marquering, H.A., Majoie, C.B.L.M., 2019. Thrombus Imaging Characteristics and Outcomes in Acute Ischemic Stroke Patients Undergoing Endovascular Treatment. Stroke 50, 2057–2064. https://doi.org/10.1161/STROKEAHA.118.024247.
Dwivedi, A., Glynn, A., Johnson, S., Duffy, S., Fereidoonnezhad, B., McGarry, P., Gilvarry, M., McCarthy, R., 2021. Measuring the Effect of Thrombosis, Thrombus Maturation and Thrombolysis on Clot Mechanical Properties in an in-Vitro Model. J. Biomech. 110731 https://doi.org/10.1016/j.jbiomech.2021.110731.
Fennell, V.S., Setlur Nagesh, S.V., Meess, K.M., Gutierrez, L., James, R.H., Springer, M.E., Siddiqui, A.H., 2018. What to do about fibrin rich "tough clots"? Comparing the Solitaire stent retriever with a novel geometric clot extractor in an in vitro stroke model. J. Neurointerv. Surg. 10, 907–910. https://doi.org/10.1136/neurintsurg-2017-013507.
Fereidoonnezhad, B., Dwivedi, A., Johnson, S., McCarthy, R., McGarry, P., 2021. Blood clot fracture properties are dependent on red blood cell and fibrin content. Acta Biomater. 127, 213–228. https://doi.org/10.1016/j.actbio.2021.03.052.
Fitzgerald Wang, S., Dai, D., Douglas, A., Gounis, M.J., Chueh, J., Puri, A.S., Layton, K.F., Ike, C., Hanel, R.A., Sauvageau, E., Aghaebrahim, A., Demchuk, A.M., Nogueira, R. G., Pereira, V.M., Kvamme, P., 2019a. Platelet-rich clots as identified by Martius Scarlett Blue staining are isodense on NCCT. J. Neurointerv. Surg. 11, 1145–1149. https://doi.org/10.1136/neurintsurg-2018-014637.Platelet-rich.
Wang Fitzgerald, S., Dai, D., Murphree, D.H., Pandit, A., Douglas, A., Rizvi, A., Kadirvel, R., Gilvarry, M., McCarthy, R., Stritt, M., Gounis, M.J., Brinjikji, W., Kallmes, D.F., Doyle, K.M., 2019b. Orbit image analysis machine learning software can be used for the histological quantification of acute ischemic stroke blood clots. PLoS One 14, 1–14. https://doi.org/10.1371/journal.pone.0225841.
Froehler, Tateshima, Duckwiler, Jhan, Gonzalez, Vinuela, Liebeskind, Saver, Villablanca, 2013. The hyperdense vessel sign on CT predicts successful recanalization with the

Merci device in acute ischemic stroke. J Neurointerv Surg 5, 289–293. https://doi.org/10.1136/neurintsurg-2012-010313.The.
Fujimoto, M., Salamon, N., Mayor, F., Yuki, I., Takemoto, K., Vinters, H.V., Viñuela, F., 2013. Characterization of arterial thrombus composition by magnetic resonance imaging in a swine stroke model. Stroke 44, 1463–1465. https://doi.org/10.1161/STROKEAHA.111.000457.
Gersh, Nagaswami, Weisel, 2009. Fibrin network structure and clot mechanical properties are altered by incorporation of erythrocytes. Thromb Haemost 102, 1169–1175. https://doi.org/10.1160/TH09-03-0199.Fibrin.
Goyal, M., Demchuk, A.M., Menon, B.K., Eesa, M., Rempel, J.L., Thornton, J., Roy, D., Jovin, T.G., Willinsky, R.A., Sapkota, B.L., Dowlatshahi, D., Frei, D.F., Kamal, N.R., Montanera, W.J., Poppe, A.Y., Ryckborst, K.J., Silver, F.L., Shuaib, A., Tampieri, D., Williams, D., Bang, O.Y., Baxter, B.W., Burns, P.A., Choe, H., Heo, J.H., Holmstedt, C.A., Jankowitz, B., Kelly, M., Linares, G., Mandzia, J.L., Shankar, J., Sohn, S. Il, Swartz, R.H., Barber, P.A., Coutts, S.B., Smith, E.E., Morrish, W.F., Weill, A., Subramaniam, S., Mitha, A.P., Wong, J.H., Lowerison, M.W., Sajobi, T.T., Hill, M.D., 2015. Randomized assessment of rapid endovascular treatment of ischemic stroke. N. Engl. J. Med. 372, 1019–1030. https://doi.org/10.1056/NEJMoa1414905.
Gunning, G.M., McArdle, K., Mirza, M., Duffy, S., Gilvarry, M., Brouwer, P.A., 2018. Clot friction variation with fibrin content; implications for resistance to thrombectomy. J. Neurointerv. Surg. 10, 34–38. https://doi.org/10.1136/neurintsurg-2016-012721.
Hashimoto, T., Hayakawa, M., Funatsu, N., Yamagami, H., Satow, T., Takahashi, J.C., Nagatsuka, K., Ishibashi-Ueda, H., Kira, J.I., Toyoda, K., 2016. Histopathologic Analysis of Retrieved Thrombi Associated with Successful Reperfusion after Acute Stroke Thrombectomy. Stroke 47, 3035–3037. https://doi.org/10.1161/STROKEAHA.116.015228.
Haussen, D.C., Rebello, L.C., Nogueira, R.G., 2015. Optimizating clot retrieval in acute stroke: The push and fluff technique for closed-cell stentrievers. Stroke 46, 2838–2842. https://doi.org/10.1161/STROKEAHA.115.010044.
Hertig, G., Zehnder, M., Woloszyk, A., Mitsiadis, T.A., Ivica, A., Weber, F.E., 2017. Iodixanol as a contrast agent in a fibrin hydrogel for endodontic applications. Front. Physiol. 8, 1–6. https://doi.org/10.3389/fphys.2017.00152.
Horie, N., Shobayashi, K., Morofuji, Y., Sadakata, E., Iki, Y., Matsunaga, Y., Kanamoto, T., Tateishi, Y., Izumo, T., Anda, T., Morikawa, M., Tsujino, A., Matsuo, T., 2019. Impact of Mechanical Thrombectomy Device on Thrombus Histology in Acute Embolic Stroke. World Neurosurg. 132, e418–e422. https://doi.org/10.1016/j.wneu.2019.08.130.
Huang, C.C., Shih, C.C., Liu, T.Y., Lee, P.Y., 2011. Assessing the Viscoelastic Properties of Thrombus Using a Solid-Sphere-Based Instantaneous Force Approach. Ultrasound Med. Biol. 37, 1722–1733. https://doi.org/10.1016/j.ultrasmedbio.2011.06.026.
Janis, A.D., Nyara, A.N., Gregory, K.W., Buckley, L.A., 2001. Characterization of an in-vitro laser thrombolysis model. Lasers Surg. Adv. Charact. Ther. Syst. XI 4244, 442. https://doi.org/10.1117/12.427833.
Janot, K., Oliveira, T.R., Fromont-Hankard, G., Annan, M., Filipiak, I., Barantin, L., Guibon, R., Duffy, S., Gilvarry, M., Cottier, J.P., Narata, A.P., 2020. Quantitative estimation of thrombus-erythrocytes using MRI. A phantom study with clot analogs and analysis by statistic regression models. J. Neurointerv. Surg. 12, 181–185. https://doi.org/10.1136/neurintsurg-2019-014950.
Johnson, S., Chueh, J., Gounis, M.J., McCarthy, R., McGarry, J.P., McHugh, P.E., Gilvarry, M., 2019. Mechanical behavior of in vitro blood clots and the implications for acute ischemic stroke treatment. J. Neurointerv. Surg. 1–6 https://doi.org/10.1136/neurintsurg-2019-015489.
Johnson, S., Duffy, S., Gunning, G., Gilvarry, M., McGarry, J.P., McHugh, P.E., 2017. Review of Mechanical Testing and Modelling of Thrombus Material for Vascular Implant and Device Design. Ann. Biomed. Eng. https://doi.org/10.1007/s10439-017-1906-5.
Johnson, S., McCarthy, R., Gilvarry, M., McHugh, P.E., McGarry, J.P., 2020. Investigating the Mechanical Behavior of Clot Analogues Through Experimental and Computational Analysis. Ann. Biomed. Eng. https://doi.org/10.1007/s10439-020-02570-5.
Jolugbo, P., Ariëns, R.A.S., 2021. Thrombus Composition and Efficacy of Thrombolysis and Thrombectomy in Acute Ischemic Stroke. Stroke 1131–1142. https://doi.org/10.1161/strokeaha.120.032810.
Jovin, T.G., Chamorro, A., Cobo, E., De Miquel, M.A., Molina, C.A., Rovira, A., San Román, L., Serena, J., Abilleira, S., Ribó, M., Millán, M., Urra, X., Cardona, P., López-Cancio, E., Tomasello, A., Castaño, C., Blasco, J., Aja, L., Dorado, L., Quesada, H., Rubiera, M., Hernández-Pérez, M., Goyal, M., Demchuk, A.M., Von Kummer, R., Gallofré, M., Dávalos, A., 2015. Thrombectomy within 8 hours after symptom onset in ischemic stroke. N. Engl. J. Med. 372, 2296–2306. https://doi.org/10.1056/NEJMoa1503780.
Kaesmacher, X.J., Boeckh-Behrens, T., Simon, S., Maegerlein, C., Kleine, J.F., Zimmer, C., Schirmer, L., Poppert, H., Huber, T., 2017. Risk of thrombus fragmentation during endovascular stroke treatment. Am. J. Neuroradiol. 38, 991–998. https://doi.org/10.3174/ajnr.A5105.
Kim, S.K., Yoon, W., Kim, T.S., Kim, H.S., Heo, T.W., Park, M.S., 2015. Histologic Analysis of Retrieved Clots in Acute Ischemic Stroke: Correlation with Stroke Etiology and Gradient-Echo MRI. AJNR 36, 1756–1762. https://doi.org/10.3174/ajnr.A4402.
Kim, O.V., Litvinov, R.I., Weisel, J.W., Alber, M.S., 2014. Structural basis for the nonlinear mechanics of fibrin networks under compression. Biomaterials 35, 6739–6749. https://doi.org/10.1016/j.biomaterials.2014.04.056.
Kirchhof, K., Welzel, T., Mecke, C., Zoubaa, S., Sartor, K., 2003. Differentiation of White, Mixed, and Red Thrombi: Value of CT in Estimation of the Prognosis of Thrombolysis—Phantom Study. Radiology 228, 126–130. https://doi.org/10.1148/radiol.2273020530.
Lam, W.A., Chaudhuri, O., Crow, A., Webster, K.D., Li, T. De, Kita, A., Huang, J., Fletcher, D.A., 2011. Mechanics and contraction dynamics of single platelets and implications for clot stiffening. Nat. Mater. 10, 61–66. https://doi.org/10.1038/nmat2903.
Liang, X., Chernysh, I., Purohit, P.K., Weisel, J.W., 2017. Phase transitions during compression and decompression of clots from platelet-poor plasma, platelet-rich plasma and whole blood. Acta Biomater. 60, 275–290. https://doi.org/10.1016/j.actbio.2017.07.011.
Liebeskind, D.S., Sanossian, N., Yong, W.H., Tsang, M.P., Moya, A.L., Zheng, D.D., Abolian, M., Kim, D., Ali, L.K., Shah, S.H., 2011. CT and MRI early vessel signs reflect clot composition in acute stroke. Stroke. https://doi.org/10.1161/STROKEAHA.110.605576.CT.
Liu, S., Bao, G., Ma, Z., Kastrup, C.J., Li, J., 2021. Fracture mechanics of blood clots: Measurements of toughness and critical length scales. Extrem. Mech. Lett. 48, 101444 https://doi.org/10.1016/j.eml.2021.101444.
Liu, Y., Reddy, A.S., Cockrum, J., Ajulufoh, M.C., Zheng, Y., Shih, A.J., Pandey, A.S., Savastano, L.E., 2020a. Standardized Fabrication Method of Human-Derived Emboli with Histologic and Mechanical Quantification for Stroke Research. J. Stroke Cerebrovasc. Dis. 29, 105205 https://doi.org/10.1016/j.jstrokecerebrovasdis.2020.105205.
Liu, Y., Zheng, Y., Reddy, A.S., Gebrezgiabhier, D., Davis, E., Cockrum, J., Gemmete, J.J., Chaudhary, N., Griauzde, J.M., Pandey, A.S., Shih, A.J., Savastano, L.E., 2020b. Analysis of human emboli and thrombectomy forces in large-vessel occlusion stroke. J. Neurosurg. 1–9 https://doi.org/10.3171/2019.12.jns192187.
Luo, Z.H., Chung, A., Choi, G., Lin, Y.H., Uchida, B.T., Pavcnik, D., Loriaux, M.M., Nesbit, G.M., Keller, F.S., Rösch, J., 2012. Creation of fibrinogen-enhanced experimental blood clots to evaluate mechanical thrombectomy devices for treatment of acute stroke: An in vitro study. J. Vasc. Interv. Radiol. 23, 1077–1083. https://doi.org/10.1016/j.jvir.2012.04.031.
Machi, P., Jourdan, F., Ambard, D., Reynaud, C., Lobotesis, K., Sanchez, M., Bonafé, A., Costalat, V., 2017. Experimental evaluation of stent retrievers' mechanical properties and effectiveness. J. Neurointerv. Surg. 9, 257–263. https://doi.org/10.1136/neurintsurg-2015-012213.
Madjidyar, J., Pineda Vidal, L., Larsen, N., Jansen, O., 2020. Influence of Thrombus Composition on Thrombectomy: ADAPT vsBalloon Guide Catheter and Stent Retriever in a Flow Model. Neuroradiology 192, 257–263. https://doi.org/10.1055/a-0998-4246.
Maegerlein, C., Friedrich, B., Berndt, M., Lucia, K.E., Schirmer, L., Poppert, H., Zimmer, C., Pelisek, J., Boeckh-Behrens, T., Kaesmacher, J., 2018. Impact of histological thrombus composition on preinterventional thrombus migration in patients with acute occlusions of the middle cerebral artery. Interv. Neuroradiol. 24, 70–75. https://doi.org/10.1177/1591019917733733.
Maekawa, K., Shibata, M., Nakajima, H., Mizutani, A., Kitano, Y., Seguchi, M., Yamasaki, M., Kobayashi, K., Sano, T., Mori, G., Yabana, T., Naito, Y., Shimizu, S., Miya, F., 2018. Erythrocyte-rich thrombus is associated with reduced number of maneuvers and procedure time in patients with acute ischemic stroke undergoing mechanical thrombectomy. Cerebrovasc. Dis. Extra 8, 39–49. https://doi.org/10.1159/000486042.
Marder, V.J., Chute, D.J., Starkman, S., Abolian, A.M., Kidwell, C., Liebeskind, D., Ovbiagele, B., Vinuela, F., Duckwiler, G., Jahan, R., Vespa, P.M., Selco, S., Rajajee, V., Kim, D., Sanossian, N., Saver, J.L., 2006. Analysis of thrombi retrieved from cerebral arteries of patients with acute ischemic stroke. Stroke 37, 2086–2093. https://doi.org/10.1161/01.STR.0000230307.03438.94.
McDonald, M.M., Archeval-Lao, J.M., Cai, C., Peng, H., Sangha, N., Parker, S.A., Wetzel, J., Riney, S.A., Cherches, M.F., Guthrie, G.J., Roper, T.C., Kawano-Castillo, J. F., Pandurengan, R., Rahbar, M.H., Grotta, J.C., 2014. Iodinated contrast does not alter clotting dynamics in acute ischemic stroke as measured by thromboelastography. Stroke 45, 462–466. https://doi.org/10.1161/STROKEAHA.113.003268.
Moftakhar, P., English, J.D., Cooke, D.L., Kim, W.T., Stout, C., Smith, W.S., Dowd, C.F., Higashida, R.T., Halbach, V.V., Hetts, S.W., 2013. Density of thrombus on admission CT predicts revascularization efficacy in large vessel occlusion acute ischemic stroke. Stroke 44, 243–245. https://doi.org/10.1161/STROKEAHA.112.674127.
Mohammaden, M.H., Haussen, D.C., Perry Da Camara, C., Pisani, L., Olive Gadea, M., Al-Bayati, A.R., Liberato, B., Rangaraju, S., Frankel, M.R., Nogueira, R.G., 2020. Hyperdense vessel sign as a potential guide for the choice of stent retriever versus contact aspiration as first-line thrombectomy strategy. J. Neurointerv. Surg. 1–6 https://doi.org/10.1136/neurintsurg-2020-016005.
Mokin, M., Morr, S., Natarajan, S.K., Lin, N., Snyder, K. V, Hopkins, L.N., Siddiqui, A.H., Levy, E.I., 2015. Thrombus density predicts successful recanalization with Solitaire stent retriever thrombectomy in acute ischemic stroke. J. Neurointerv. Surg. 7, 104 LP – 107. https://doi.org/10.1136/neurintsurg-2013-011017.
Mönch, S., Boeckh-Behrens, T., Berndt, M., Maegerlein, C., Wunderlich, S., Zimmer, C., Friedrich, B., 2019. Angiographic Baseline Proximal Thrombus Appearance of M1/M2 Occlusions in Mechanical Thrombectomy. Clin. Neuroradiol. https://doi.org/10.1007/s00062-019-00863-4.
Münster, S., Jawerth, L.M., Leslie, B.A., Weitz, J.I., Fabry, B., Weitz, D.A., 2013. Strain history dependence of the nonlinear stress response of fibrin and collagen networks. Proc. Natl. Acad. Sci. U. S. A. 110, 12197–12202. https://doi.org/10.1073/pnas.1222787110.
New, P.F.J., Aronow, S., 1976. Attenuation measurements of whole blood and blood fractions in computed tomography. Radiology 121, 635–640. https://doi.org/10.1148/121.3.635.

Niesten, J.M., Van Der Schaaf, I.C., Van Dam, L., Vink, A., Vos, J.A., Schonewille, W.J., De Bruin, P.C., Mali, W.P.T.M., Velthuis, B.K., 2014. Histopathologic composition of cerebral thrombi of acute stroke patients is correlated with stroke subtype and thrombus attenuation. PLoS One 9, 12–14. https://doi.org/10.1371/journal.pone.0088882.

Patel, T.R., Waqas, M., Tso, M., Dmytriw, A., Mokin, M., Kolega, J., Tomaszewski, J., Levy, E.I., Davies, J.M., Snyder, K.V., Siddiqui, A.H., Tutino, V.M., 2021. Increased Perviousness on CT for Acute Ischemic Stroke is Associated with Fibrin / Platelet-Rich Clots. AJNR 1–8.

Piechocka, I.K., Bacabac, R.G., Potters, M., Mackintosh, F.C., Koenderink, G.H., 2010. Structural hierarchy governs fibrin gel mechanics. Biophys. J. 98, 2281–2289. https://doi.org/10.1016/j.bpj.2010.01.040.

Powers, W.J., Rabinstein, A.A., Ackerson, T., Adeoye, O.M., Bambakidis, N.C., Becker, K., Biller, J., Brown, M., Demaerschalk, B.M., Hoh, B., Jauch, E.C., Kidwell, C.S., Leslie-Mazwi, T.M., Ovbiagele, B., Scott, P.A., Sheth, K.N., Southerland, A.M., Summers, D. V., Tirschwell, D.L., 2019. Guidelines for the early management of patients with acute ischemic stroke: 2019 update to the 2018 guidelines for the early management of acute ischemic stroke a guideline for healthcare professionals from the American Heart Association/American Stroke A. Stroke. https://doi.org/10.1161/STR.0000000000000211.

Rossi, R., Molina, S., Mereuta, O.M., Douglas, A., Fitzgerald, S., Tierney, C., Pandit, A., Brennan, P., Power, S., O'Hare, A., Gilvarry, M., McCarthy, R., Magoufis, G., Tsivgoulis, G., Nagy, A., Vadász, Á., Jood, K., Redfors, P., Nordanstig, A., Ceder, E., Dunker, D., Carlqvist, J., Psychogios, K., Szikora, I., Tatlisumak, T., Rentzos, A., Thornton, J., Doyle, K.M., 2021. Does prior administration of rtPA influence acute ischemic stroke clot composition? Findings from the analysis of clots retrieved with mechanical thrombectomy from the RESTORE registry. J. Neurol. https://doi.org/10.1007/s00415-021-10758-5.

Santos, E.M.M., Marquering, H.A., Den Blanken, M.D., Berkhemer, O.A., Boers, A.M.M., Yoo, A.J., Beenen, L.F., Treurniet, K.M., Wismans, C., Van Noort, K., Lingsma, H.F., Dippel, D.W.J., Van Der Lugt, A., Van Zwam, W.H., Roos, Y.B.W.E.M., Van Oostenbrugge, R.J., Niessen, W.J., Majoie, C.B., 2016a. Thrombus Permeability Is Associated with Improved Functional Outcome and Recanalization in Patients with Ischemic Stroke. Stroke 47, 732–741. https://doi.org/10.1161/STROKEAHA.115.011187.

Santos, E.M.M., Niessen, W.J., Yoo, A.J., Berkhemer, O.A., Beenen, L.F., Majoie, C.B., Marquering, H.A., Fransen, P.S.S., Beumer, D., Van Den Berg, L.A., Lingsma, H.F., Schonewille, W.J., Vos, J.A., Nederkoorn, P.J., Wermer, M.J.H., Van Walderveen, M. A.A., Staals, J., Hofmeijer, J., Van Oostayen, J.A., Nijeholt, G.J.L.À., Boiten, J., Brouwer, P.A., Emmer, B.J., De Bruijn, S.F., Van Dijk, L.C., Kappelle, L.J., Lo, R.H., Van Dijk, E.J., De Vries, J., De Kort, P.L.M., Van Den Berg, J.S.P., Van Hasselt, B.A.A. M., Aerden, L.A.M., Dallinga, R.J., Visser, M.C., Bot, J.C.J., Vroomen, P.C., Eshghi, O., Schreuder, T.H.C.M.L., Heijboer, R.J.J., Keizer, K., Tielbeek, A.V., Den Hertog, H.M., Gerrits, D.G., Van Den Berg-Vos, R.M., Karas, G.B., Steyerberg, E.W., Flach, H.Z., Sprengers, M.E.S., Jenniskens, S.F.M., Beenen, L.F.M., Van Den Berg, R., Koudstaal, P.J., Van Zwam, W.H., Roos, Y.B.W.E.M., Van Der Lugt, A., Van Oostenbrugge, R.J., Majoie, C.B.L.M., Dippel, D.W.J., 2016b. Automated entire thrombus density measurements for robust and comprehensive thrombus characterization in patients with acute ischemic stroke. PLoS One 11, 1–16. https://doi.org/10.1371/journal.pone.0145641.

Santos, E.M.M., Yoo, A.J., Beenen, L.F., Berkhemer, O.A., den Blanken, M.D., Wismans, C., Niessen, W.J., Majoie, C.B., Marquering, H.A., 2016c. Observer variability of absolute and relative thrombus density measurements in patients with acute ischemic stroke. Neuroradiology 58, 133–139. https://doi.org/10.1007/s00234-015-1607-4.

Saver, J.L., Goyal, M., Bonafe, A., Diener, H.C., Levy, E.I., Pereira, V.M., Albers, G.W., Cognard, C., Cohen, D.J., Hacke, W., Jansen, O., Jovin, T.G., Mattle, H.P., Nogueira, R.G., Siddiqui, A.H., Yavagal, D.R., Baxter, B.W., Devlin, T.G., Lopes, D.K., Reddy, V.K., De Rochemont, R.D.M., Singer, O.C., Jahan, R., 2015. Stent-retriever thrombectomy after intravenous t-PA vs. t-PA alone in stroke. N. Engl. J. Med. 372, 2285–2295. https://doi.org/10.1056/NEJMoa1415061.

Shin, J.W., Jeong, H.S., Kwon, H.J., Song, K.S., Kim, J., 2018. High red blood cell composition in clots is associated with successful recanalization during intra-arterial thrombectomy. PLoS One 13, 1–13. https://doi.org/10.1371/journal.pone.0197492.

Simons, N., Mitchell, P., Dowling, R., Gonzales, M., Yan, B., 2015. Thrombus composition in acute ischemic stroke: A histopathological study of thrombus extracted by endovascular retrieval. J. Neuroradiol. 42, 86–92. https://doi.org/10.1016/j.neurad.2014.01.124.

Sporns, P.B., Hanning, U., Schwindt, W., Velasco, A., Buerke, B., Cnyrim, C., Minnerup, J., Heindel, W., Jeibmann, A., Niederstadt, T., 2017. Ischemic Stroke: Histological Thrombus Composition and Pre-Interventional CT Attenuation Are Associated with Intervention Time and Rate of Secondary Embolism. Cerebrovasc. Dis. 44, 344–350. https://doi.org/10.1159/000481578.

Sporns, P.B., Krähling, H., Psychogios, M.N., Jeibmann, A., Minnerup, J., Broocks, G., Meyer, L., Brehm, A., Wildgruber, M., Fiehler, J., Kniep, H., Hanning, U., 2020. Small thrombus size, thrombus composition, and poor collaterals predict pre-interventional thrombus migration. J. Neurointerv. Surg. 1–6 https://doi.org/10.1136/neurintsurg-2020-016228.

Staessens, S., De Meyer, S.F., 2020. Thrombus heterogeneity in ischemic stroke. Platelets. https://doi.org/10.1080/09537104.2020.1748586.

Staessens, S., Denorme, F., François, O., Desender, L., Dewaele, T., Vanacker, P., Deckmyn, H., Vanhoorelbeke, K., Andersson, T., De Meyer, S.F., 2020. Structural analysis of ischemic stroke thrombi: Histological indications for therapy resistance. Haematologica 105, 498–507. https://doi.org/10.3324/haematol.2019.219881.

Tolhuisen, M.L., Enthoven, J., Santos, E.M.M., Niessen, W.J., Beenen, L.F.M., Dippel, D. W.J., van der Lugt, A., van Zwam, W.H., Roos, Y.B.W.E.M., van Oostenbrugge, R.J., Majoie, C.B.L.M., Marquering, H.A., 2017. The Effect of Non-contrast CT Slice Thickness on Thrombus Density and Perviousness Assessment. In: Cardoso, M.J., Arbel, T., Gao, F., Kainz, B., van Walsum, T., Shi, K., Bhatia, K.K., Peter, R., Vercauteren, T., Reyes, M., Dalca, A., Wiest, R., Niessen, W., Emmer, B.J. (Eds.), Molecular Imaging, Reconstruction and Analysis of Moving Body Organs, and Stroke Imaging and Treatment. Springer International Publishing, Cham, pp. 168–175.

Tutwiler, V., Peshkova, A.D., Andrianova, I.A., Khasanova, D.R., Weisel, J.W., Litvinov, R.I., 2017. Contraction of blood clots is impaired in acute ischemic stroke. Arterioscler. Thromb. Vasc. Biol. 37, 271–279. https://doi.org/10.1161/ATVBAHA.116.308622.

Tutwiler, V., Singh, J., Litvinov, R.I., Bassani, J.L., Purohit, P.K., Weisel, J.W., 2020. Rupture of blood clots : Mechanics and pathophysiology. Sci. Adv. 6, eabc0496. https://doi.org/10.1126/sciadv.abc0496.

Tynngård, N., Lindahl, T., Ramström, S., Berlin, G., 2006. Effects of different blood components on clot retraction analysed by measuring elasticity with a free oscillating rheometer. Platelets 17, 545–554. https://doi.org/10.1080/09537100600759238.

Van Der Marel, K., Chueh, J.Y., Brooks, O.W., King, R.M., Marosfoi, M.G., Langan, E.T., Carniato, S.L., Gounis, M.J., Nogueira, R.G., Puri, A.S., 2016. Quantitative assessment of device-clot interaction for stent retriever thrombectomy. J. Neurointerv. Surg. 8, 1278–1282. https://doi.org/10.1136/neurintsurg-2015-012209.

van Kempen, T.H.S., Donders, W.P., van de Vosse, F.N., Peters, G.W.M., 2016. A constitutive model for developing blood clots with various compositions and their nonlinear viscoelastic behavior. Biomech. Model. Mechanobiol. 15, 279–291. https://doi.org/10.1007/s10237-015-0686-9.

Velasco Gonzalez, A., Buerke, B., Görlich, D., Fobker, M., Rusche, T., Sauerland, C., Meier, N., Jeibmann, A., McCarthy, R., Kugel, H., Sporns, P., Faldum, A., Paulus, W., Heindel, W., 2020. Clot Analog Attenuation in Non-contrast CT Predicts Histology: an Experimental Study Using Machine Learning. Transl. Stroke Res. 11, 940–949. https://doi.org/10.1007/s12975-019-00766-z.

Weafer, F.M., Duffy, S., Machado, I., Gunning, G., Mordasini, P., Roche, E., McHugh, P. E., Gilvarry, M., 2019. Characterization of strut indentation during mechanical thrombectomy in acute ischemic stroke clot analogs. J. Neurointerv. Surg. 11, 891–897. https://doi.org/10.1136/neurintsurg-2018-014601.

Wei, L., Zhu, Y., Deng, J., Li, Y., Li, M., Lu, H., Zhao, Y., 2021. Visualization of Thrombus Enhancement on Thin-Slab Maximum Intensity Projection of CT Angiography: An Imaging Sign for Predicting Stroke Source and Thrombus Compositions. Radiology 298, 374–381. https://doi.org/10.1148/radiol.2020201548.

Wintermark, M., Sanelli, P.C., Albers, G.W., Bello, J.A., Derdeyn, C.P., Hetts, S.W., Johnson, M.H., Kidwell, C.S., Lev, M.H., Liebeskind, D.S., Rowley, H.A., Schaefer, P. W., Sunshine, J.L., Zaharchuk, G., Meltzer, C.C., 2013. Imaging Recommendations for Acute Stroke and Transient Ischemic Attack Patients. J. Am. Coll. Radiol. 10, 828–832. https://doi.org/10.1016/j.jacr.2013.06.019.

Yamamoto, N., Satomi, J., Tada, Y., Harada, M., Izumi, Y., Nagahiro, S., Kaji, R., 2015. Two-layered susceptibility vessel sign on 3-tesla T2*-weighted imaging is a predictive biomarker of stroke subtype. Stroke 46, 269–271. https://doi.org/10.1161/STROKEAHA.114.007227.

Ye, G., Cao, R., Lu, J., Qi, P., Hu, S., Chen, K., Tan, T., Chen, J., Wang, D., 2021. Histological composition behind CT-based thrombus density and perviousness in acute ischemic stroke. Clin. Neurol. Neurosurg. 207, 106804 https://doi.org/10.1016/j.clineuro.2021.106804.

Ye, G., Qi, P., Chen, K., Tan, T., Cao, R., Chen, J., Lu, J., Wang, D., 2020. Risk of secondary embolism events during mechanical thrombectomy for acute ischemic stroke: A single-center study based on histological analysis. Clin. Neurol. Neurosurg. 193, 105749 https://doi.org/10.1016/j.clineuro.2020.105749.

Yoo, A.J., Andersson, T., 2017. Thrombectomy in acute ischemic stroke: Challenges to procedural success. J. Stroke 19, 121–130. https://doi.org/10.5853/jos.2017.00752.

Yuki, I., Kan, I., Vinters, H.V., Kim, R.H., Golshan, A., Vinuela, F.A., Sayre, J.W., Murayama, Y., Vinuela, F., 2012. The impact of thromboemboli histology on the performance of a mechanical thrombectomy device. Am. J. Neuroradiol. 33, 643–648. https://doi.org/10.3174/ajnr.A2842.